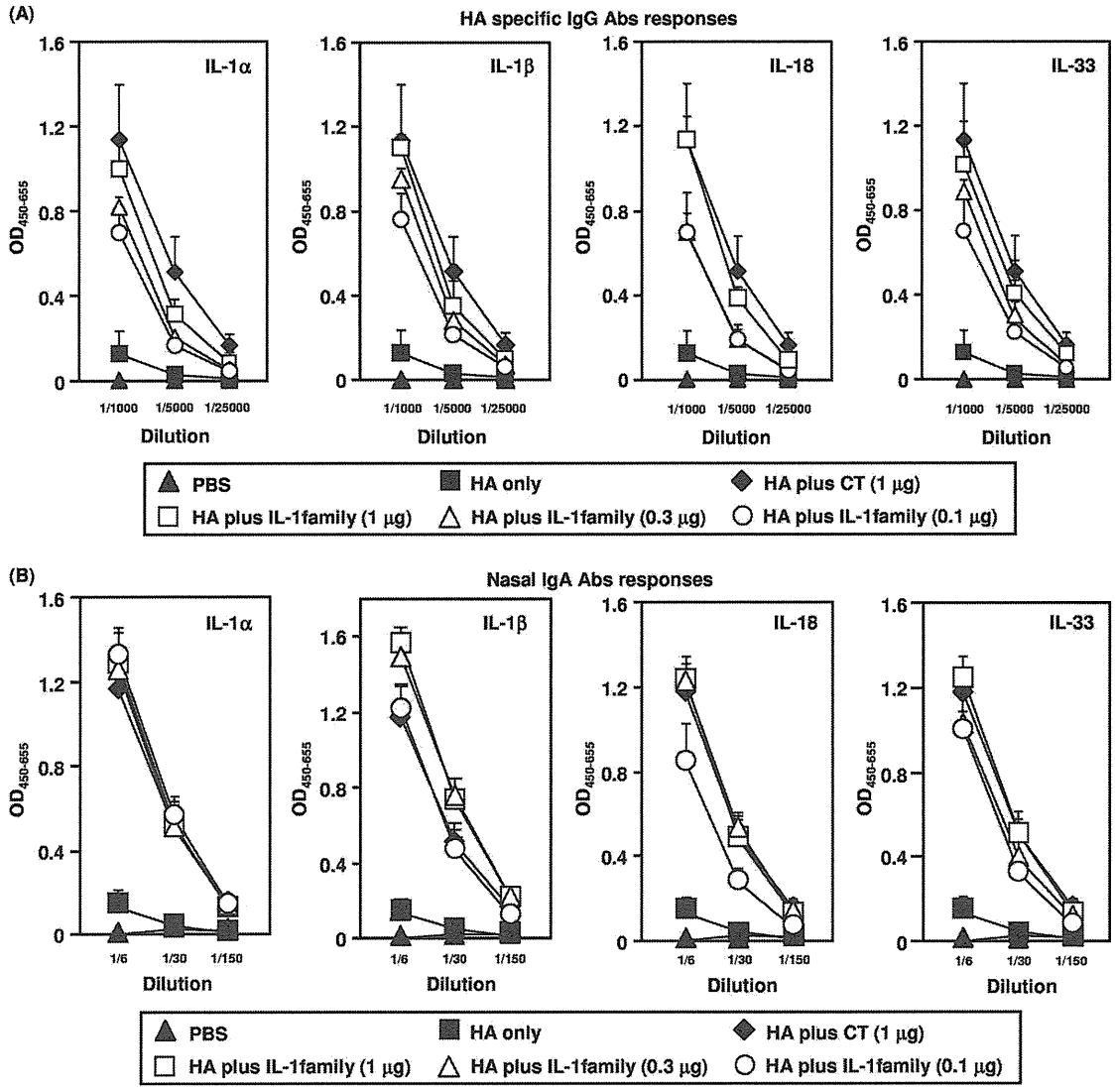

FIG. 2. Dose-response relationship for induction of rHA-specific Ab responses by nasal immunization with rHA plus an IL-1 family cytokine. BALB/c mice were immunized intranasally at 0 and 28 days with rHA alone, rHA plus CT (1 μg/mouse), or rHA plus an IL-1 family cytokine (0.1, 0.3, or 1 μg/mouse). (A) Plasma was collected 14 days after the final immunization and analyzed by ELISA for rHA-specific IgG, at dilutions of 1/1,000, 1/5,000, and 1/250,000. (B) Nasal washes were collected 14 days after the final immunization and analyzed by ELISA for rHA-specific sIgA, at dilutions of 1/6, 1/30, and 1/150. Data are presented as means ± SEM (n = 5).

significantly higher IgG1 and IgG2a Ab responses than those immunized with rHA alone. These results indicate that nasal administration of IL-1 family cytokines has the potential to induce potent rHA-specific systemic IgG Abs, as well as IgG1 and IgG2a Ab responses. We then studied the rHA-specific sIgA response in mucosal secretions (i.e., in saliva, nasal washes, fecal extracts, and vaginal washes) induced by the 26 IL cytokines (Fig. 1B). For these 26 IL cytokines, IL-1 family cytokines induced the highest mucosal sIgA Ab responses in salivary, nasal, fecal, and vaginal mucosal secretions (Fig. 1B). Taken together, these results indicate that nasal immunization with IL-1 family cytokines effectively induced rHA-specific Ab responses in both systemic and mucosal immune compartments, suggesting that IL-1 family cytokines might be effective mucosal vaccine adjuvants.

Dose-response relationship of IL-1 family cytokines as mucosal vaccine adjuvants for induction of rHA-specific Ab responses. To determine the dose-response relationship of IL-1 family cytokines as mucosal vaccine adjuvants to induce rHA-specific IgG and sIgA Ab responses, mice were immunized intranasally with rHA plus 0.1, 0.3, or 1 μg of each IL-1 family cytokine (Fig. 2). Immunization with rHA plus the IL-1 family cytokines induced rHA-specific IgG in plasma in a dose-dependent manner. Even rHA plus the lowest dose (0.1 μg) of IL-1 family cytokines induced IgG to levels significantly higher than those induced by rHA alone (Fig. 2A). Importantly, the use of 1 μg of IL-1 family cytokines as an adjuvant resulted in

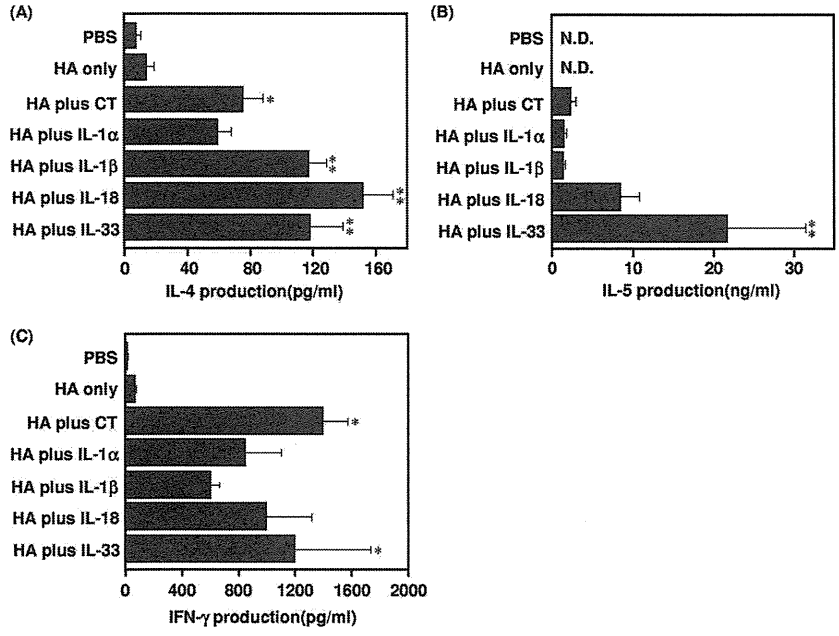

FIG. 3. Cytokine responses induced by nasal immunization with rHA plus IL-1 family cytokines. BALB/c mice were immunized intranasally at 0 and 28 days with rHA alone, rHA plus CT, or rHA plus an IL-1 family cytokine. Fourteen days after the final immunization, splenocytes from each group were cultured with 10 μg rHA/ml. Culture supernatants were harvested after a 3-day incubation and then assayed for rHA-specific IL-4 (A), IL-5 (B), and IFN-γ (C), using a Bio-Plex multiplex cytokine assay. Data are presented as means ± SEM ($n = 5$). *, $P < 0.05$; **, $P < 0.01$ compared to the value for the rHA-treated group. N.D., not done.

strong rHA-specific IgG Ab responses equivalent to those elicited by CT, which is one of the most potent mucosal vaccine adjuvants (Fig. 2A). Furthermore, the level of rHA-specific sIgA induced by rHA plus 0.1 μg of each IL-1 family cytokine in nasal secretions was significantly higher than that induced by rHA alone (Fig. 2B). The level of rHA-specific nasal sIgA induced in mice immunized intranasally with rHA plus 0.3 μg of each IL-1 family cytokine was equivalent to that observed in mice treated with 1 μg CT. Taken together, these results clearly indicate that nasal immunization with an IL-1 family cytokine as a mucosal vaccine adjuvant induced dose-dependent levels of both rHA-specific IgG and sIgA Abs in the mucosal and systemic immune compartments.

Induction of rHA-specific Th1- and Th2-type responses after nasal administration of IL-1 family cytokines as mucosal vaccine adjuvants. To evaluate the ability of IL-1 family cytokines to boost rHA-specific cytokine responses induced by mucosal immunization, splenocytes from mice that had been immunized intranasally with rHA alone, rHA plus CT, or rHA plus an IL-1 family cytokine were restimulated *in vitro* with rHA and then assayed for Th1 (IFN-γ) and Th2 (IL-4 and IL-5) cytokines (Fig. 3). Splenocytes from mice immunized with rHA alone did not show significant cytokine production compared to those from PBS-treated mice. Consistent with the IgG subclass results (Fig. 1A), mice immunized with IL-1 family cytokines had higher levels of IL-4 and IL-5 (Th2-associated sIgA-enhancing cytokines) than mice given rHA alone. In particular, the highest levels of IL-4 and IL-5 were detected in splenocytes of mice immunized with rHA plus IL-18 or IL-33, and these responses were significantly higher than those in splenocytes of mice immunized with CT. It was also noteworthy that IFN-γ, a Th1 cytokine, was induced in mice immunized intranasally with rHA plus an IL-1 family cytokine. Thus, IL-1 family cytokines might induce CTL responses when administered nasally. These results show that as mucosal vaccine adjuvants, IL-1α, IL-1β, IL-18, and IL-33 elicit both Th1- and Th2-type cytokine responses.

***In vivo* CTL induction by nasal immunization with rHA plus IL-1 family cytokines as mucosal vaccine adjuvants.** Virus clearance is known to require strong Th1-polarized immune responses characterized by IFN-γ production and CTL responses in the systemic compartment. To investigate the ability of IL-1 family cytokines to act as mucosal vaccine adjuvants and to induce rHA-specific Th1/CTL immune responses, we measured H-2K^d/HA$_{240–248}$ tetramer$^+$ CD8$^+$ T cells (Fig. 4A) and H-2K^d/HA$_{240–248}$-specific IFN-γ-secreting cells (Fig. 4B) in splenocytes from mice that had been immunized intranasally with rHA alone, rHA plus CT, or rHA plus an IL-1 family cytokine. The level of H-2K^d/HA$_{240–248}$ tetramer$^+$ CD8$^+$ T cells induced by rHA plus IL-1β was found to be similar to that induced by rHA alone, but the level induced by rHA plus IL-1α, IL-18, or IL-33 was significantly greater than that induced by rHA alone (Fig. 4A). Furthermore, the level of functionally active H-2K^d/HA$_{240–248}$-specific IFN-γ-secreting cells induced by rHA plus IL-1α, IL-18, or IL-33 was the same as or greater than that in mice intranasally immunized with rHA plus CT (Fig. 4B). Taken together, these results indicate that the IL-1 family cytokines IL-1α, IL-18 and IL-33 induce high-avidity CD8$^+$ CTLs. Therefore, intranasally administered IL-1α, IL-18, and IL-33 might be useful adjuvants for development of an effective mucosal influenza vaccine.

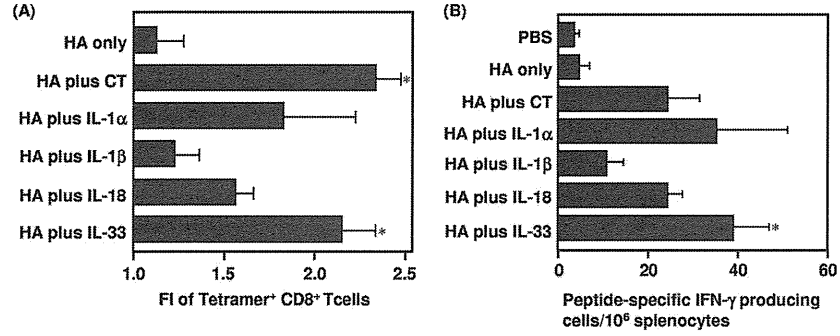

FIG. 4. Measurement of H-2K^d/HA$_{240-248}$ tetramer$^+$ CD8$^+$ T cells and H-2K^d/HA$_{240-248}$-specific IFN-γ-secreting cells in the spleen after nasal immunization with rHA plus an IL-1 family cytokine. BALB/c mice were immunized intranasally at 0 and 28 days with rHA alone, rHA plus CT, or rHA plus an IL-1 family cytokine. Fourteen days after the final immunization, splenocytes from immunized mice were harvested and stimulated with H-2K^d-restricted class I HA peptide at a final concentration of 10 μg total peptide/ml. (A) For detection of H-2K^d/HA$_{240-248}$ tetramer$^+$ CD8$^+$ T cells, splenocytes from immunized mice were cultured in medium containing a CTL epitope peptide (HA$_{240-248}$; IYSTVASSL) plus 10 U human IL-2/ml for 7 days, stained for CD8, and analyzed for tetramer-binding cells by flow cytometry. FI, fluorescence intensity. (B) After 24 h of incubation, IFN-γ-producing cells were measured by an ELISPOT assay. Data are presented as means ± SEM ($n = 5$). *, $P < 0.05$ compared to the value for the rHA-treated group.

Histopathological changes due to IL-1 family cytokines administered intranasally as mucosal vaccine adjuvants. Although enterotoxin-based adjuvants show strong mucosal immunity-inducing ability, they have significant toxic side effects on the central nervous system due to the presence of a specific receptor, GM1 ganglioside, which is highly expressed in neuronal tissue (39). To evaluate the *in vivo* toxicity of IL-1 family cytokines, histopathological changes in nasal tissues of mice given 1 μg of IL-1 family cytokines were investigated. No histological changes indicative of severe inflammation or membrane barrier disruption were observed in the nasal cavities of mice nasally administrated 1 μg of an IL-1 family cytokine (Fig. 5A). In particular, there was no evidence of massive accumulations of mononuclear cells around the airways and blood vessels or of infiltrates in the nasal tissues for all mice examined. Importantly, mice immunized intranasally with IL-1 family cytokines did not induce the goblet cell hyperplasia observed in patients with asthma and chronic obstructive pulmonary disease. Furthermore, Luna staining revealed that IL-1 family cytokine-treated mice did not develop infiltration of Luna-stained eosinophils into the nasal septum (Fig. 5B). Although further evaluation is required, these results indicate that the toxicity of IL-1 family cytokines is likely to be relatively low.

Antiviral immune response to influenza virus infection in mice after nasal immunization with IL-1 family cytokines as mucosal vaccine adjuvants. To determine the level of protection against viral infection provided by IL-1 family cytokines, BALB/c mice were immunized intranasally with 1 μg PR8 HA alone or with 1 μg of an IL-1 family cytokine on days 0 and 28. The immunized mice were then challenged with 256 HAU of mouse-adapted PR8 virus 14 days after the final immunization. The survival and weight of the infected mice were observed every other day (Fig. 6). All mice in the group receiving PBS alone and 86% of the mice immunized with PR8 HA alone died within 7 days of infection. In contrast, mice immunized intranasally with PR8 HA plus an IL-1 family cytokine showed a marked increase in survival (Fig. 6A). Notably, mice immunized with PR8 HA plus IL-1β or IL-18 had 100% survival 14 days after challenge, though with a slight loss of body weight (Fig. 6B). These results indicate that IL-1 family cytokines are potent nasal vaccine adjuvants for providing protection against viral infection.

Role of MCs in rHA-specific immune responses induced by nasal immunization with rHA plus IL-1 family cytokines. MCs are localized predominantly at the interface between the host and the environment (i.e., skin and mucosal surfaces). Recent reports have demonstrated the importance of IL-18-mediated MC activation for host defense, including innate sensing of pathogens (35) and recruitment of DCs and T lymphocytes to sites of inflammation. These findings prompted us to investigate whether MCs have a significant role in the immune response induced by IL-1 family cytokines as mucosal vaccine adjuvants. Hence, we examined MC-dependent rHA-specific systemic IgG and mucosal sIgA Ab responses induced by IL-1 family cytokine adjuvants. For this study, we compared the induction of specific Ab responses in MC-deficient (*W/W^v*) and WT mice immunized intranasally with rHA plus an IL-1 family cytokine (Fig. 7A and B). Both WT and *W/W^v* mice immunized with rHA had only minimal rHA-specific IgG Ab responses. However, rHA plus an IL-1 family cytokine induced significant rHA-specific IgG Ab responses in WT mice. *W/W^v* mice immunized with rHA plus IL-1α, IL-1β, or IL-33 also had significant rHA-specific IgG Ab responses (Fig. 7A), suggesting that IL-1α, IL-1β, and IL-33 act in an MC-independent manner. In contrast, the rHA-specific IgG Ab response induced in *W/W^v* mice by IL-18 was considerably lower than that in WT mice (Fig. 7A). Similar results were found for mucosal sIgA Ab responses: a significant response was seen with rHA plus IL-1α, IL-1β, or IL-33 in both WT and *W/W^v* mice, and a decreased response was seen with rHA plus IL-18 in *W/W^v* mice compared to WT mice (Fig. 7B). We then compared IL-4, IL-5, IL-2, and IFN-γ production in WT and *W/W^v* mice immunized with rHA plus IL-1 family cytokines (Fig. 7C). WT mice immunized with rHA plus IL-1 family cytokines showed significantly more rHA-specific IL-4, IL-5, IL-2, and IFN-γ production than did WT mice immunized with rHA alone. In contrast, the responses induced by rHA plus IL-18 were sig-

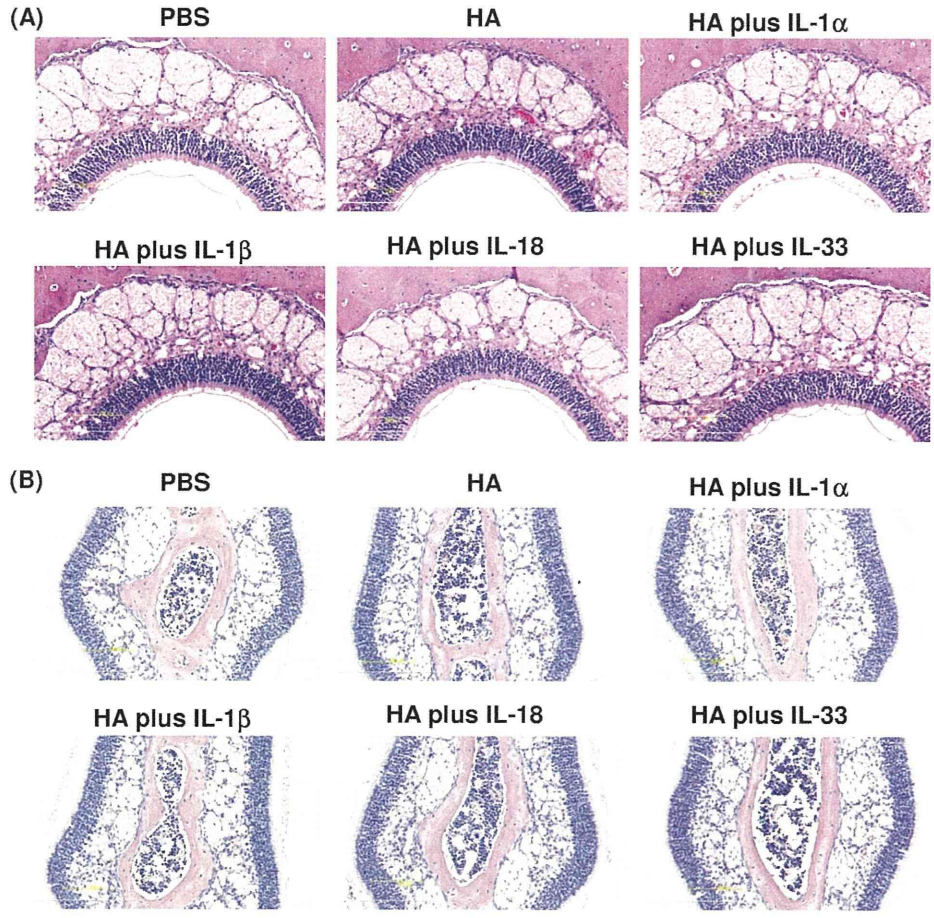

FIG. 5. Histopathological analysis of the nasal cavities of mice immunized intranasally with IL-1 family cytokines. Frontal cross sections of the nasal cavities of mice were taken after two administrations of PBS, rHA alone, or rHA plus an IL-1 family cytokine. Sections were prepared and stained with H&E (A) or Luna stain (B) to assess pathological changes. Overall views of the nasal epithelium (A) and of Luna-stained eosinophils in the nasal septum (B) are shown.

nificantly reduced in *W/W*^{v} mice. In addition, although rHA-specific IL-2, IL-4, and IL-5 production in *W/W*^{v} mice immunized with rHA plus IL-33 was comparable to that in WT mice, the rHA-specific IFN-γ response was significantly reduced in *W/W*^{v} mice. Collectively, these results indicate that MCs have a crucial role in the rHA-specific immune response induced by nasal immunization with rHA plus IL-18. In particular, MCs appear to have an important role in regulating rHA-specific

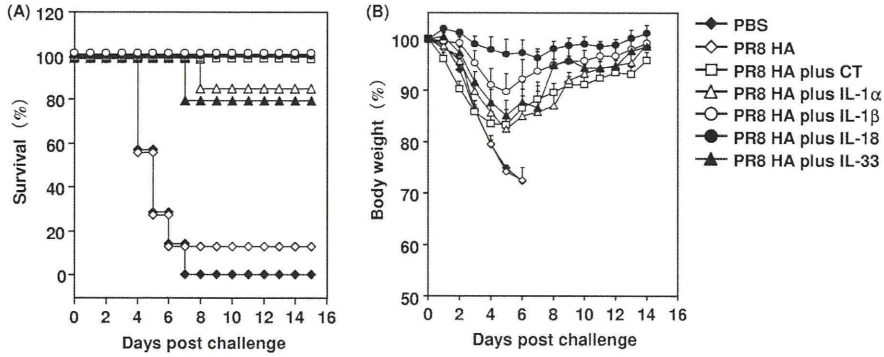

FIG. 6. Protection of BALB/c mice against lethal influenza virus infection by IL-1 family cytokine adjuvants. BALB/c mice were immunized intranasally at 0 and 28 days with rHA alone, rHA plus CT (1 μg/mouse), or rHA plus an IL-1 family cytokine (1 μg/mouse). Fourteen days after the final immunization, mice were intranasally infected with 256 HAU of influenza virus A/PR/8/34. Mice were monitored for survival (A) and weight loss (B) for 14 days after infection. The results are expressed as percent survival (A) and percent initial body weight (B). Data are presented as means ± SEM (n = 4 to 7).

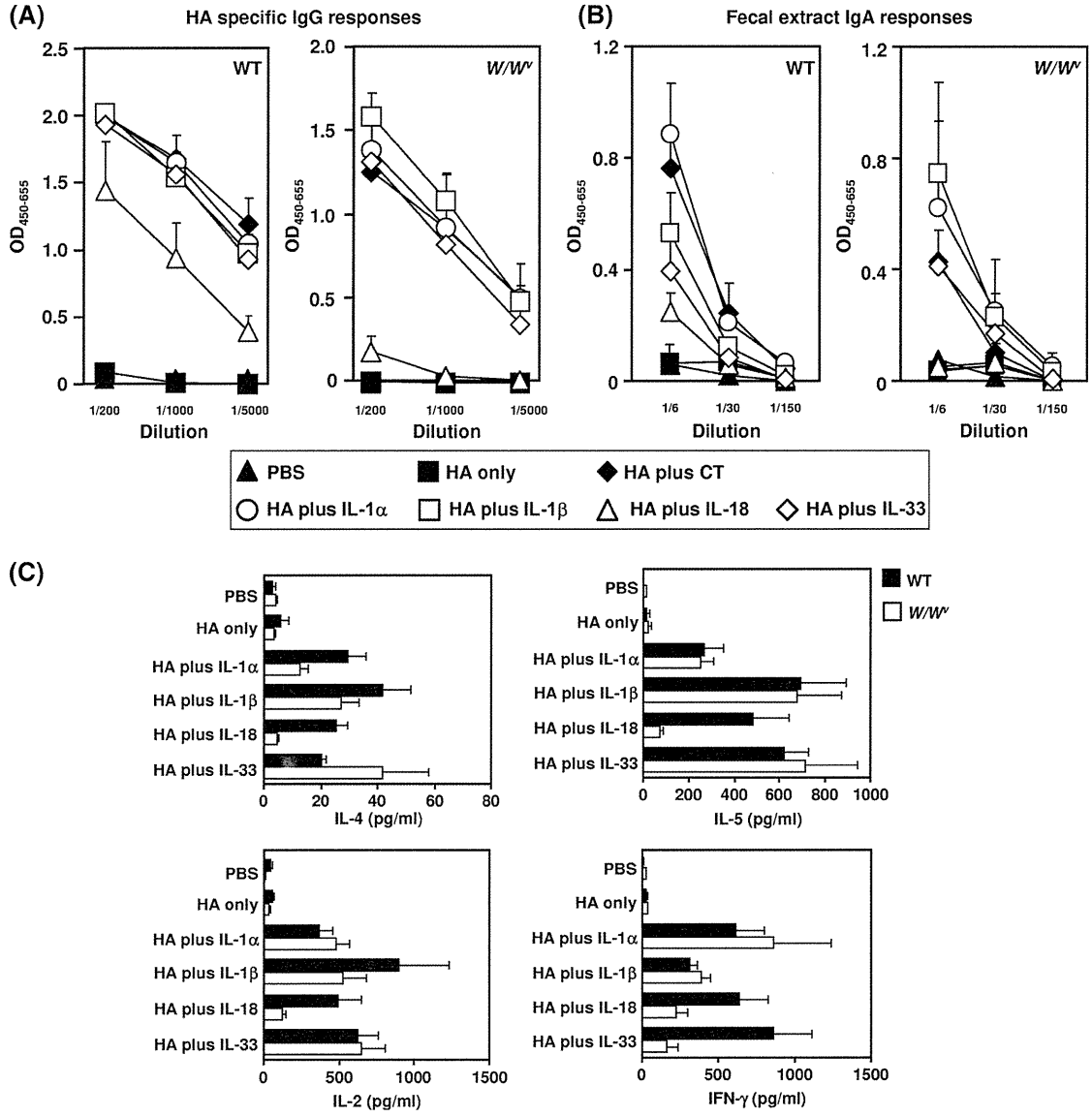

FIG. 7. Role of MCs in induction of rHA-specific immune responses by nasal immunization with rHA plus IL-1 family cytokines. WBB6F1 *W/Wv* and WT mice were immunized intranasally at 0 and 28 days with rHA alone, rHA plus CT (1 μg/mouse), or rHA plus an IL-1 family cytokine (1 μg/mouse). Plasma and fecal extracts were collected 14 days after the final immunization and analyzed by ELISA for rHA-specific IgG in plasma (A) and rHA-specific sIgA in fecal extracts (B). (C) Also, 14 days after immunization, splenocytes from each group of WBB6F1 *W/Wv* and WT mice were cultured with 10 μg rHA/ml. Culture supernatants were harvested after a 3-day incubation, and rHA-specific cytokine production (IL-4, IL-5, IL-2, and IFN-γ) in the culture supernatants was analyzed using a Bio-Plex multiplex cytokine assay. Data are presented as means ± SEM (n = 5).

IFN-γ-mediated Th1-type immunity in mice immunized with rHA plus IL-33 as a mucosal vaccine adjuvant.

DISCUSSION

Of the 26 different IL cytokines studied here, intranasal immunization with rHA plus an IL-1 family cytokine (IL-1α, IL-1β, IL-18, and IL-33) induced the highest levels of rHA-specific systemic IgG. High levels of sIgA were also observed in the mucosa of IL-1 family cytokine-treated mice. However, IL-12 and IL-15 have been reported to promote systemic and mucosal immunity to intramucosally coadministered protein Ags (8, 45), although more frequent immunization was required to produce adjuvant activity. The apparent discrepancy concerning the adjuvant activity of IL-12 and IL-15 in this study and previous reports may be due to differences in immunization regimens and vaccine doses.

For IL-1 family cytokines, we showed that intranasal administration of rHA plus IL-1α, IL-18, or IL-33 induced higher levels of $CD8^+$ CTLs than intranasal administration of rHA alone, whereas the level induced by rHA plus IL-1β was similar to that induced by rHA alone. In agreement with these results, IL-1β has been reported to have a pivotal role in development of Th2-type immune responses (20). A previous report by

Shibuya et al. (36) showed that IL-1α is necessary for optimal Th1 development and IFN-γ secretion in BALB/c mice. In addition, Karupiah et al. (46) showed that IL-18 and IL-12p40 regulate cellular immune responses through $CD8^+$ T-cell activation. Thus, our data are in agreement with previous reports that IL-1α and IL-18 play a pivotal role in inducing Th1-type immune responses. Furthermore, there have been a few reports on the potential of IL-33 to induce a Th1-type immune response (37). In the present study, we showed that of the IL-1 family cytokines, IL-33 induced the highest levels of CTL and IFN-γ^+ cells. We are currently investigating the mechanism of IL-33 in Th1/CTL immunity.

We found that intranasal coadministration of influenza vaccine with IL-1 family cytokines provided protection against influenza viral infection, with IL-1β and IL-18 providing complete protection. It is known that nasal secretions containing locally produced sIgA and serum-derived IgG Abs contribute to forming a first line of defense for combating influenza viral infections (42, 44). Therefore, the prophylactic effects of IL-1 family cytokines may be due mainly to Ab-mediated immunity against influenza virus. Furthermore, previous studies have pointed out the importance of influenza-specific $CD8^+$ CTLs for host recovery from lethal influenza virus infections and protection against further infection (7, 15). Although the mechanism by which IL-18 provided complete protection against influenza remains to be elucidated, high-avidity $CD8^+$ CTLs induced by IL-1α, IL-18, or IL-33 probably confer protection against influenza viral infection. Recently, a requirement for NK cells or NKT cells for control of influenza virus infections was identified (10, 13). Since IL-18 is known to regulate NK and NKT cell activity (4, 38), it is possible that restimulation of these cells may have resulted in the reduction in virus replication and morbidity observed after viral challenge. We are currently investigating the involvement of these cell subsets in the induction of protection against influenza virus by IL-18.

Unfortunately, potent adjuvant action is often correlated with increased toxicity, as exemplified by CT adjuvant, which although it is potent is too toxic for human use. Therefore, one of the major challenges in adjuvant research is to gain potency while minimizing toxicity (17). Intranasal administration of 1 μg of an IL-1 family cytokine for four consecutive days has been shown to induce asthma-like symptoms, including airway hyperresponsiveness and goblet cell hyperplasia in the lungs (26). In contrast, in this study, we found that mice immunized intranasally with IL-1 family cytokines did not exhibit acute toxicity, i.e., there was no cytokine-induced mortality, no obvious weight loss, no abnormal behavior, and no histopathological changes. In addition, use of 0.1 μg of an IL-1 family cytokine as a nasal vaccine adjuvant was still effective at inducing systemic IgG and nasal sIgA Ab responses. Thus, although further safety evaluation is needed, our findings indicate a broad therapeutic utility for IL-1 family cytokines when used as adjuvants for mucosal vaccination.

To develop optimal vaccines for clinical applications, it is important to understand their mechanism of action on the immune system in terms of efficacy as well as safety (23). The present study demonstrates that the enhanced mucosal vaccine adjuvant effect of IL-18 operates via an MC-dependent mechanism. The rHA-specific immune response induced by intranasally administered rHA plus IL-18 in WT mice was significantly reduced in W/W^v mice. In addition, the level of the rHA-specific IFN-γ response in mice intranasally immunized with rHA plus IL-33 was minimal in W/W^v mice. Although studies are needed on the role of MCs in generation of Ag-specific immunity, the studies reported here show that MCs have a role in the effect of IL-18 as an adjuvant and in augmentation of the CTL response induced by IL-33 as a nasal vaccine adjuvant. MC activators (e.g., compound 48/80) have been reported to stimulate protective immune responses against infections (28, 32). In addition, these immune responses are correlated with DC trafficking and lymphocyte recruitment to draining lymph nodes (DLN). Nakae et al. (30) suggested that MC-derived tumor necrosis factor alpha (TNF-α) is required for enhanced recruitment of lymphocytes and DCs to DLN. MC-dependent induction of IL-18 mucosal vaccine adjuvant activity may involve these types of processes. In agreement with this possibility, the IL-18 receptor was highly expressed on the surfaces of MCs but not in nasal passage-associated lymphoid tissue $CD11c^+$ DCs, and IL-18 induced robust TNF-α and IL-6 production from MCs in a concentration-dependent manner *in vitro* (unpublished data). Although further studies are required, IL-18 appeared to exhibit MC-dependent adjuvant activity that was not directly regulated by DC functions, such as DC migration and DC activation.

In summary, IL-1 family cytokines used as mucosal vaccine adjuvants induced two layers of protective immunity when administered intranasally with an influenza virus vaccine Ag, indicating that they may be suitable for use in antiviral nasal vaccines.

ACKNOWLEDGMENTS

We have no financial conflicts of interest.

This study was supported in part by grants-in-aid for scientific research from the Ministry of Education, Culture, Sports, Science and Technology of Japan and from the Japan Society for the Promotion of Science (JSPS). This study was also supported in part by Health Labor Sciences Research Grants from the Ministry of Health, Labor and Welfare of Japan and by Health Sciences Research Grants for Research on Publicly Essential Drugs and Medical Devices from the Japan Health Sciences Foundation.

REFERENCES

1. **Ada, G.** 2001. Vaccines and vaccination. N. Engl. J. Med. **345:**1042–1053.
2. **Ahlers, J. D., I. M. Belyakov, S. Matsui, and J. A. Berzofsky.** 2001. Mechanisms of cytokine synergy essential for vaccine protection against viral challenge. Int. Immunol. **13:**897–908.
3. **Arend, W. P., G. Palmer, and C. Gabay.** 2008. IL-1, IL-18, and IL-33 families of cytokines. Immunol. Rev. **223:**20–38.
4. **Baxevanis, C. N., A. D. Gritzapis, and M. Papamichail.** 2003. In vivo antitumor activity of NKT cells activated by the combination of IL-12 and IL-18. J. Immunol. **171:**2953–2959.
5. **Belyakov, I. M., and J. D. Ahlers.** 2008. Functional CD8+ CTLs in mucosal sites and HIV infection: moving forward toward a mucosal AIDS vaccine. Trends Immunol. **29:**574–585.
6. **Belyakov, I. M., J. D. Ahlers, B. Y. Brandwein, P. Earl, B. L. Kelsall, B. Moss, W. Strober, and J. A. Berzofsky.** 1998. The importance of local mucosal HIV-specific CD8(+) cytotoxic T lymphocytes for resistance to mucosal viral transmission in mice and enhancement of resistance by local administration of IL-12. J. Clin. Invest. **102:**2072–2081.
7. **Bender, B. S., T. Croghan, L. Zhang, and P. A. Small, Jr.** 1992. Transgenic mice lacking class I major histocompatibility complex-restricted T cells have delayed viral clearance and increased mortality after influenza virus challenge. J. Exp. Med. **175:**1143–1145.
8. **Boyaka, P. N., M. Marinaro, R. J. Jackson, S. Menon, H. Kiyono, E. Jirillo, and J. R. McGhee.** 1999. IL-12 is an effective adjuvant for induction of mucosal immunity. J. Immunol. **162:**122–128.

9. **Boyaka, P. N., M. Ohmura, K. Fujihashi, T. Koga, M. Yamamoto, M. N. Kweon, Y. Takeda, R. J. Jackson, H. Kiyono, Y. Yuki, and J. R. McGhee.** 2003. Chimeras of labile toxin one and cholera toxin retain mucosal adjuvanticity and direct Th cell subsets via their B subunit. J. Immunol. **170:**454–462.
10. **Cerwenka, A., and L. L. Lanier.** 2001. Natural killer cells, viruses and cancer. Nat. Rev. Immunol. **1:**41–49.
11. **Croft, M.** 2009. The role of TNF superfamily members in T-cell function and diseases. Nat. Rev. Immunol. **9:**271–285.
12. **De Gregorio, E., U. D'Oro, and A. Wack.** 2009. Immunology of TLR-independent vaccine adjuvants. Curr. Opin. Immunol. **21:**339–345.
13. **Diana, J., and A. Lehuen.** 2009. NKT cells: friend or foe during viral infections? Eur. J. Immunol. **39:**3283–3291.
14. **Dinarello, C. A.** 2009. Immunological and inflammatory functions of the interleukin-1 family. Annu. Rev. Immunol. **27:**519–550.
15. **Doherty, P. C., J. M. Riberdy, and G. T. Belz.** 2000. Quantitative analysis of the CD8+ T-cell response to readily eliminated and persistent viruses. Philos. Trans. R. Soc. Lond. B Biol. Sci. **355:**1093–1101.
16. **Galli, S. J., S. Nakae, and M. Tsai.** 2005. Mast cells in the development of adaptive immune responses. Nat. Immunol. **6:**135–142.
17. **Griffin, M. R., M. M. Braun, and K. J. Bart.** 2009. What should an ideal vaccine postlicensure safety system be? Am. J. Public Health **99**(Suppl. 2)**:**S345–S350.
18. **Haynes, B. F., and R. J. Shattock.** 2008. Critical issues in mucosal immunity for HIV-1 vaccine development. J. Allergy Clin. Immunol. **122:**3–9.
19. **Heib, V., M. Becker, T. Warger, G. Rechtsteiner, C. Tertilt, M. Klein, T. Bopp, C. Taube, H. Schild, E. Schmitt, and M. Stassen.** 2007. Mast cells are crucial for early inflammation, migration of Langerhans cells, and CTL responses following topical application of TLR7 ligand in mice. Blood **110:** 946–953.
20. **Helmby, H., and R. K. Grencis.** 2004. Interleukin 1 plays a major role in the development of Th2-mediated immunity. Eur. J. Immunol. **34:**3674–3681.
21. **Holmgren, J., and C. Czerkinsky.** 2005. Mucosal immunity and vaccines. Nat. Med. **11:**S45–S53.
22. **Hubbell, J. A., S. N. Thomas, and M. A. Swartz.** 2009. Materials engineering for immunomodulation. Nature **462:**449–460.
23. **Ishii, K. J., T. Kawagoe, S. Koyama, K. Matsui, H. Kumar, T. Kawai, S. Uematsu, O. Takeuchi, F. Takeshita, C. Coban, and S. Akira.** 2008. TANK-binding kinase-1 delineates innate and adaptive immune responses to DNA vaccines. Nature **451:**725–729.
24. **Kayamuro, H., Y. Abe, Y. Yoshioka, K. Katayama, T. Nomura, T. Yoshida, K. Yamashita, T. Yoshikawa, Y. Kawai, T. Mayumi, T. Hiroi, N. Itoh, K. Nagano, H. Kamada, S. Tsunoda, and Y. Tsutsumi.** 2009. The use of a mutant TNF-alpha as a vaccine adjuvant for the induction of mucosal immune responses. Biomaterials **30:**5869–5876.
25. **Kayamuro, H., Y. Yoshioka, Y. Abe, K. Katayama, T. Yoshida, K. Yamashita, T. Yoshikawa, T. Hiroi, N. Itoh, Y. Kawai, T. Mayumi, H. Kamada, S. Tsunoda, and Y. Tsutsumi.** 2009. TNF superfamily member, TL1A, is a potential mucosal vaccine adjuvant. Biochem. Biophys. Res. Commun. **384:** 296–300.
26. **Kondo, Y., T. Yoshimoto, K. Yasuda, S. Futatsugi-Yumikura, M. Morimoto, N. Hayashi, T. Hoshino, J. Fujimoto, and K. Nakanishi.** 2008. Administration of IL-33 induces airway hyperresponsiveness and goblet cell hyperplasia in the lungs in the absence of adaptive immune system. Int. Immunol. **20:**791–800.
27. **Marinaro, M., H. F. Staats, T. Hiroi, R. J. Jackson, M. Coste, P. N. Boyaka, N. Okahashi, M. Yamamoto, H. Kiyono, H. Bluethmann, K. Fujihashi, and J. R. McGhee.** 1995. Mucosal adjuvant effect of cholera toxin in mice results from induction of T helper 2 (Th2) cells and IL-4. J. Immunol. **155:**4621–4629.
28. **McLachlan, J. B., C. P. Shelburne, J. P. Hart, S. V. Pizzo, R. Goyal, R. Brooking-Dixon, H. F. Staats, and S. N. Abraham.** 2008. Mast cell activators: a new class of highly effective vaccine adjuvants. Nat. Med. **14:**536–541.
29. **Mutsch, M., W. Zhou, P. Rhodes, M. Bopp, R. T. Chen, T. Linder, C. Spyr, and R. Steffen.** 2004. Use of the inactivated intranasal influenza vaccine and the risk of Bell's palsy in Switzerland. N. Engl. J. Med. **350:**896–903.
30. **Nakae, S., H. Suto, M. Kakurai, J. D. Sedgwick, M. Tsai, and S. J. Galli.** 2005. Mast cells enhance T cell activation: importance of mast cell-derived TNF. Proc. Natl. Acad. Sci. U. S. A. **102:**6467–6472.
31. **Neutra, M. R., and P. A. Kozlowski.** 2006. Mucosal vaccines: the promise and the challenge. Nat. Rev. Immunol. **6:**148–158.
32. **Pulendran, B., and S. J. Ono.** 2008. A shot in the arm for mast cells. Nat. Med. **14:**489–490.
33. **Reddy, S. T., M. A. Swartz, and J. A. Hubbell.** 2006. Targeting dendritic cells with biomaterials: developing the next generation of vaccines. Trends Immunol. **27:**573–579.
34. **Reed, S. G., S. Bertholet, R. N. Coler, and M. Friede.** 2009. New horizons in adjuvants for vaccine development. Trends Immunol. **30:**23–32.
35. **Sasaki, Y., T. Yoshimoto, H. Maruyama, T. Tegoshi, N. Ohta, N. Arizono, and K. Nakanishi.** 2005. IL-18 with IL-2 protects against Strongyloides venezuelensis infection by activating mucosal mast cell-dependent type 2 innate immunity. J. Exp. Med. **202:**607–616.
36. **Shibuya, K., D. Robinson, F. Zonin, S. B. Hartley, S. E. Macatonia, C. Somoza, C. A. Hunter, K. M. Murphy, and A. O'Garra.** 1998. IL-1 alpha and TNF-alpha are required for IL-12-induced development of Th1 cells producing high levels of IFN-gamma in BALB/c but not C57BL/6 mice. J. Immunol. **160:**1708–1716.
37. **Smithgall, M. D., M. R. Comeau, B. R. Yoon, D. Kaufman, R. Armitage, and D. E. Smith.** 2008. IL-33 amplifies both Th1- and Th2-type responses through its activity on human basophils, allergen-reactive Th2 cells, iNKT and NK cells. Int. Immunol. **20:**1019–1030.
38. **Son, Y. I., R. M. Dallal, R. B. Mailliard, S. Egawa, Z. L. Jonak, and M. T. Lotze.** 2001. Interleukin-18 (IL-18) synergizes with IL-2 to enhance cytotoxicity, interferon-gamma production, and expansion of natural killer cells. Cancer Res. **61:**884–888.
39. **Spangler, B. D.** 1992. Structure and function of cholera toxin and the related Escherichia coli heat-labile enterotoxin. Microbiol. Rev. **56:**622–647.
40. **Stelekati, E., R. Bahri, O. D'Orlando, Z. Orinska, H. W. Mittrucker, R. Langenhaun, M. Glatzel, A. Bollinger, R. Paus, and S. Bulfone-Paus.** 2009. Mast cell-mediated antigen presentation regulates CD8+ T cell effector functions. Immunity **31:**665–676.
41. **Surh, C. D., and J. Sprent.** 2008. Homeostasis of naive and memory T cells. Immunity **29:**848–862.
42. **Tamura, S., Y. Ito, H. Asanuma, Y. Hirabayashi, Y. Suzuki, T. Nagamine, C. Aizawa, and T. Kurata.** 1992. Cross-protection against influenza virus infection afforded by trivalent inactivated vaccines inoculated intranasally with cholera toxin B subunit. J. Immunol. **149:**981–988.
43. **Toka, F. N., C. D. Pack, and B. T. Rouse.** 2004. Molecular adjuvants for mucosal immunity. Immunol. Rev. **199:**100–112.
44. **Tumpey, T. M., M. Renshaw, J. D. Clements, and J. M. Katz.** 2001. Mucosal delivery of inactivated influenza vaccine induces B-cell-dependent heterosubtypic cross-protection against lethal influenza A H5N1 virus infection. J. Virol. **75:**5141–5150.
45. **Wang, X., X. Zhang, Y. Kang, H. Jin, X. Du, G. Zhao, Y. Yu, J. Li, B. Su, C. Huang, and B. Wang.** 2008. Interleukin-15 enhance DNA vaccine elicited mucosal and systemic immunity against foot and mouth disease virus. Vaccine **26:**5135–5144.
46. **Wang, Y., G. Chaudhri, R. J. Jackson, and G. Karupiah.** 2009. IL-12p40 and IL-18 play pivotal roles in orchestrating the cell-mediated immune response to a poxvirus infection. J. Immunol. **183:**3324–3331.

Journal of Virology

Enhanced Growth of Influenza Vaccine Seed Viruses in Vero Cells Mediated by Broadening the Optimal pH Range for Virus Membrane Fusion

Shin Murakami, Taisuke Horimoto, Mutsumi Ito, Ryo Takano, Hiroaki Katsura, Masayuki Shimojima and Yoshihiro Kawaoka

J. Virol. 2012, 86(3):1405. DOI: 10.1128/JVI.06009-11.
Published Ahead of Print 16 November 2011.

JVI
Journals.ASM.org

Enhanced Growth of Influenza Vaccine Seed Viruses in Vero Cells Mediated by Broadening the Optimal pH Range for Virus Membrane Fusion

Shin Murakami,[a]* Taisuke Horimoto,[a,b] Mutsumi Ito,[a] Ryo Takano,[a,c] Hiroaki Katsura,[a] Masayuki Shimojima,[a] and Yoshihiro Kawaoka[a,c,d,e]

Division of Virology, Department of Microbiology and Immunology, Institute of Medical Science, University of Tokyo, Tokyo, Japan[a]; Department of Veterinary Microbiology, Graduate School of Agricultural and Life Sciences, University of Tokyo, Tokyo, Japan[b]; ERATO Infection-Induced Host Responses Project, Japan Science and Technology Agency, Saitama, Japan[c]; International Research Center for Infectious Diseases, Institute of Medical Science, University of Tokyo, Tokyo, Japan[d]; and Influenza Research Institute, Department of Pathological Sciences, School of Veterinary Medicine, University of Wisconsin—Madison, Madison, Wisconsin, USA[e]

Vaccination is one of the most effective preventive measures to combat influenza. Prospectively, cell culture-based influenza vaccines play an important role for robust vaccine production in both normal settings and urgent situations, such as during the 2009 pandemic. African green monkey Vero cells are recommended by the World Health Organization as a safe substrate for influenza vaccine production for human use. However, the growth of influenza vaccine seed viruses is occasionally suboptimal in Vero cells, which places limitations on their usefulness for enhanced vaccine production. Here, we present a strategy for the development of vaccine seed viruses with enhanced growth in Vero cells by changing an amino acid residue in the stem region of the HA2 subunit of the hemagglutinin (HA) molecule. This mutation optimized the pH for HA-mediated membrane fusion in Vero cells and enhanced virus growth 100 to 1,000 times in the cell line, providing a promising strategy for cell culture-based influenza vaccines.

Although several antivirals against influenza viruses, including neuraminidase (NA) inhibitors, have been developed and used worldwide, vaccination is still considered one of the most effective preventive measures to combat influenza (12, 23). Currently, most conventional influenza vaccines are produced from viruses grown in embryonated chicken eggs. However, the limited capacity of the egg-dependent vaccine supply could be problematic in terms of securing enough doses when facing a pandemic situation, such as occurred in 2009, or in the event of a pandemic originating from a highly pathogenic avian virus, such as an H5N1 virus. In these situations, cell culture-based systems could play an important role for robust vaccine production (4).

Presently, cell culture-based inactivated influenza vaccines are in clinical trials or have been approved for use in some countries (1, 7, 8, 13, 19). This approach has considerable advantages over egg-based vaccines because (i) it can lead to more rapid and larger-scale vaccine production (10); (ii) it may avoid the potential for selecting variants adapted for chicken eggs, which alters virus antigenicity (18); (iii) selection of high-yield vaccine seed viruses is needed for egg-based production; and (iv) it does not contain allergic components of eggs (16). Due to these advantages, the World Health Organization (WHO) has recommended the establishment of mammalian cell culture-based vaccines (41).

Several cell lines are currently approved for cell culture-based influenza vaccine production. One of them, the African green monkey Vero cell line, has a good track record for the production of other viral vaccines for human use (e.g., polio and rabies vaccines) (26). In their long history, Vero cells have proven safe for vaccine production, so the WHO now recommends this cell line as an alternative substrate for influenza vaccine production (2). However, since seed viruses for seasonal inactivated vaccines occasionally grow suboptimally in Vero cells, seed viruses that grow well in Vero cells must be carefully selected for robust vaccine production (37). Here, we present a strategy for the development of vaccine seed viruses with enhanced growth in Vero cells by changing an amino acid residue in the hemagglutinin (HA) stem region. This approach could help overcome shortages in the influenza vaccine supply in emergency pandemic situations.

MATERIALS AND METHODS

Cells. African green monkey Vero WCB cells, approved for use in human vaccine production (38), were maintained in Dulbecco's modified Eagle's minimal essential medium (DMEM) with 10% fetal calf serum and antibiotics. Madin-Darby canine kidney (MDCK) cells were grown in Eagle's minimal essential medium (MEM) with 5% newborn calf serum and antibiotics. The cells were maintained at 37°C in 5% CO_2.

Virus adaptation to Vero cells. The A/Puerto Rico/8/34 [PR8(UW)] strain (27, 31) was generated by using reverse genetics (29) and propagated in 10-day-old embryonated chicken eggs for 2 days at 37°C, after which the allantoic fluids containing viruses were harvested and stored at −80°C. PR8 virus was inoculated into Vero cells in bovine serum albumin (BSA) (0.3%)-containing MEM with tosylsulfonyl phenylalanyl chloromethyl ketone (TPCK)-trypsin (1 μg/ml). Three to 4 days after infection, virus-containing supernatants were collected and inoculated into fresh Vero cells at 1:100 or 1:1,000 dilution. After 11 passages, virus-containing supernatant was collected and stored at −80°C. Stock virus titers were determined by using a plaque assay in MDCK cells.

Received 15 August 2011 Accepted 8 November 2011
Published ahead of print 16 November 2011
Address correspondence to Taisuke Horimoto, ahorimo@mail.ecc.u-tokyo.ac.jp, or Yoshihiro Kawaoka, kawaoka@ims.u-yokyo.ac.jp.
* Present address: Department of Microbiology and Immunology, University of Texas Medical Branch, Galveston, Texas, USA.

doi:10.1128/JVI.06009-11

TABLE 1 Comparison of amino acid sequences between wild-type PR8 and PR8-Vero viruses

Virus gene	Accession no.	Amino acid position	Residue	
			PR8 WT	PR8-Vero
HA (HA2)	AB671289[a]	117	N	D (4)[b]
NA	AB671290	255	N	Y (4)
PB2	AB671295	740	D	N (2)

[a] GenBank accession number of wild-type sequence.
[b] Number of clones that acquired the mutation out of four clones.

Virus gene sequencing. Viral RNAs were extracted from supernatants by using a commercial kit (QiaAmp viral RNA isolation kit; Qiagen) and were converted to cDNAs by using reverse transcriptase (SuperScript III; Invitrogen) and primers based on the consensus sequences of the 3-prime ends of the RNA segments for the H1N1 viruses. The full-length cDNAs were then PCR amplified with *Pfu*Ultra DNA polymerase (Stratagene) and PR8-specific primer pairs for each segment. The amplified cDNAs were cloned by using the Zero Blunt TOPO PCR Cloning Kit (Invitrogen). For each segment, four clones were sequenced by using PR8-specific primers. Primer sequences are available upon request.

Construction of mutant viruses. We used our previously produced series of PolI constructs, derived from PR8(UW), for reverse genetics (15, 27) and PolI plasmids containing the HA and NA genes derived from A/Kawasaki/173/2001 (H1N1; Kawasaki173; GenBank accession numbers AB671296 and AB671297 for HA and NA, respectively), A/Kawasaki/UTK-4/09 (H1N1; UTK-4; GenBank accession numbers AB671291 and AB671292 for HA and NA, respectively), A/California/04/09 (H1N1; CA04; GenBank accession numbers FJ966082.1 and FJ966084.1 for HA and NA, respectively), and A/Yokohama/2013/03 (H3N2; Yok2013; GenBank accession numbers AB671293 and AB671294 for HA and NA, respectively) (20, 30). To generate HA, NA, and PB2 mutants, PolI plasmids expressing the HA, NA, and PB2 genes of PR8, Kawasaki173, UTK-4, CA04, or Yok2013 were used as templates for site-directed mutagenesis by the inverse PCR method. PR8 mutants and PR8 backbone 6:2 reassortants containing the six internal segments of PR8 and the HA and NA segments of seasonal or pandemic viruses were generated by using reverse genetics (29).

Virus replication in Vero and MDCK cells. Virus was inoculated into Vero or MDCK cell monolayers at a multiplicity of infection (MOI) of 0.01 PFU/cell with MEM containing BSA and 1.0 μg/ml TPCK-trypsin and incubated at 37°C (for PR8, PR8/Kawasaki173 6:2 reassortant, PR8/UTK-4 6:2 reassortant, PR8/CA04 6:2 reassortant, and PR8/Yok2013 6:2 reassortant viruses) or at 33°C (for PR8/CA04 6:2 reassortant viruses). Viruses in the culture supernatants were collected at a given number of hours postinfection (p.i.) and then titrated by use of an MDCK plaque assay to determine the virus titers.

Cell fusion assay. The cell fusion assay was performed as previously described (33) with some modifications. Briefly, Vero cells were transfected with PR8 HA or mutant HA (N117DHA2) expression plasmids (pCAGGS-PR8HA or pCAGGS-PR8HA2N117D, respectively), as well as with a green fluorescent protein (GFP) expression plasmid (pCAGGS-GFP) to conveniently visualize fused cells under a fluorescence microscope. After transfection, the cells were incubated at 37°C for 24 h. The cells were then washed several times with Mg^{2+}- and Ca^{2+}-containing phosphate-buffered saline (PBS^-) and treated with 5 μg/ml of TPCK-trypsin for 5 min at 37°C. The trypsin was then inactivated by washing with PBS^+ containing FCS. To initiate cell fusion, the cells were treated with acidic PBS (adjusted with citric acid) for 1 min and then incubated in FCS-containing medium at 37°C for 30 min. Fused cells were observed under a fluorescence microscope (Biozero; Keyence).

Comparison of endosomal pHs. Comparisons of endosomal pHs between Vero and MDCK cells were performed as previously described (25, 35), with some modifications. Briefly, Vero and MDCK cells were incubated with Alexa Fluor 647 (30 μg/ml; Invitrogen)- and Oregon green 488 (250 μg/ml; Invitrogen)-conjugated dextran and incubated for 15 min at 37°C. After incubation, the cells were immediately placed on ice and washed 5 times with ice-cold PBS^+, and the intensities of the Alexa Fluor 647 and Oregon green 488 were measured by using confocal microscopy (LSM 510; Carl Zeiss) in five microscopic fields for each sample. The Oregon green 488/Alexa Fluor 647 intensity ratio was then calculated.

Statistical analysis. All comparisons of the infectivity titers of each virus and the intensity ratio for Oregon green 488/Alexa Fluor 647 relied on Student's *t* test with two-tailed analysis to determine significant differences.

RESULTS

Adaptation of PR8 virus for Vero cells. To obtain a virus that grows to a high titer in Vero cells, we performed serial passages of the PR8 virus in the cell line. Initially, wild-type (WT) PR8 virus-infected Vero cells showed an ambiguous cytopathic effect. After eight passages, however, we observed a clear cytopathic effect in Vero cells. After the 11th passage, we collected the virus (referred to as the PR8-Vero virus). We then compared wild-type and PR8-Vero virus titers in the supernatants of infected Vero cells. Wild-type virus grew to 2.0×10^4 PFU/ml, whereas PR8-Vero virus grew to 1.9×10^9 PFU/ml. These data suggest that PR8-Vero virus possesses mutations that enhance its replication in Vero cells.

Identification of mutations responsible for Vero cell adaptation. To identify the mutation(s) responsible for PR8 adaptation to Vero cells, the virus genome was sequenced. The cDNAs of the PR8-Vero virus were cloned into plasmids, and the sequences of four clones for each segment were read. As shown in Table 1, PR8-Vero virus contained mutations in the HA (4/4 clones), NA (4/4 clones), and PB2 (2/4 clones) genes, and all of these mutations caused amino acid changes. No mutations were identified in any of the other gene segments. Next, we introduced the mutation(s) into wild-type PR8 by using reverse genetics and examined the growth kinetics of the mutants (Fig. 1). The D740N PB2 PR8 mutant virus grew similarly to wild-type PR8, whereas the N255Y NA mutation augmented viral growth to 8.5×10^5 PFU/ml. Interestingly, the N117D HA2 mutant virus grew to the highest titer (6.3×10^8 PFU/ml). Both the N255Y NA and N117D HA2 mutations caused virus to grow to a level comparable to that of PR8-

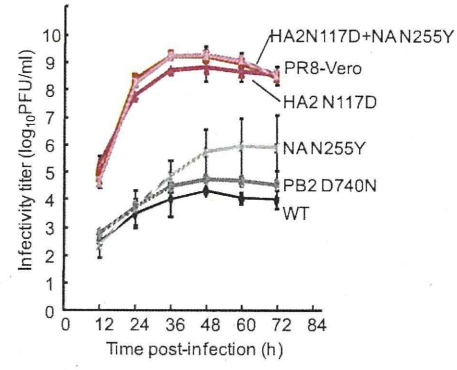

FIG 1 Growth of Vero cell-adapted PR8 viruses in Vero cells. Viral titers of wild-type PR8 (WT), Vero cell-adapted PR8 (PR8-Vero), and mutants possessing amino acid substitution(s) observed in PR8-Vero viruses were determined at 12, 24, 36, 48, 60, and 72 h p.i. at an MOI of 0.01. The data are reported as mean titers with standard deviations for three independent experiments.

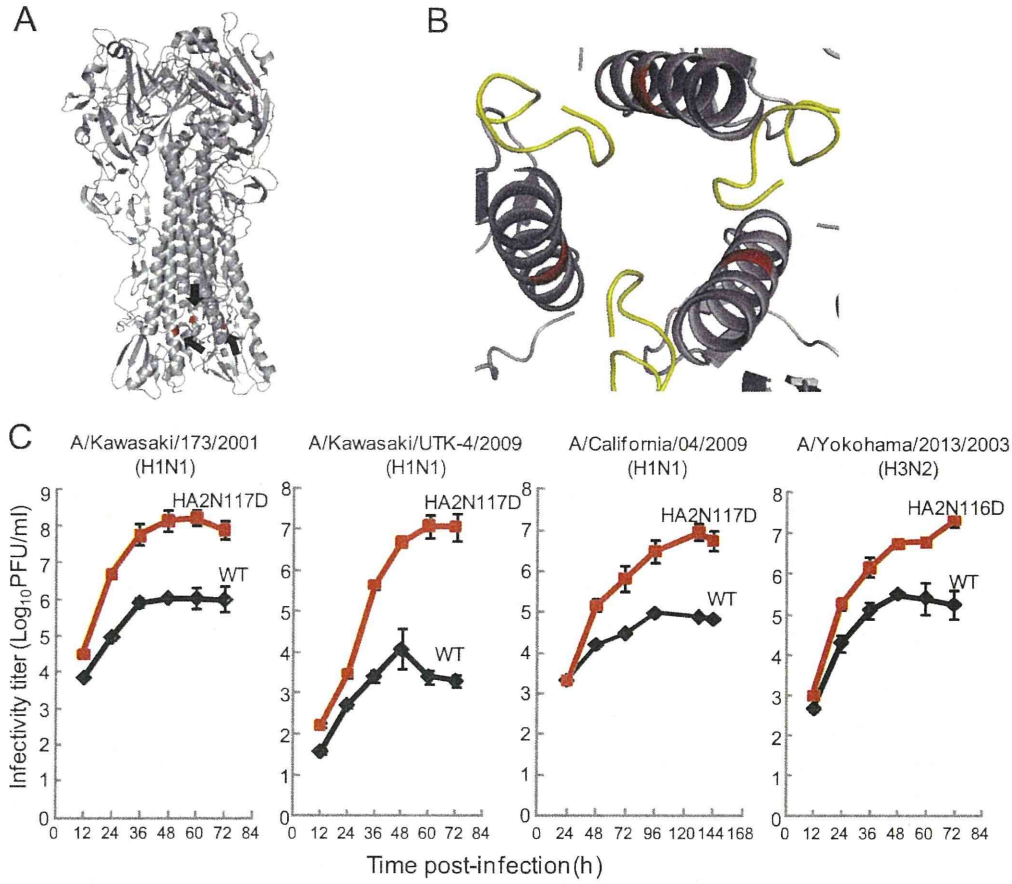

FIG 2 Growth enhancement of vaccine seed-like viruses mediated by the HA2 N117D (N116D) mutation. (A) Location of the HA2 N117 residue on the three-dimensional (3D) structure of A/Puerto Rico/8/34 (PDB:1RU7). HA2 117 is colored red. (B) Close-up view of the region indicated by arrows in panel A. The view is from the globular head of the HA trimer. The locations of HA2 N117 and fusion peptides are colored as follows: HA2 117, red; fusion peptide, yellow. (C) Growth of PR8 background 6:2 reassortant viruses possessing the HA2 N117D (N116D for H3) mutation. The viral titers of the parental 6:2 reassortant (WT) and mutants were determined at the indicated times after infection at an MOI of 0.01. The data are reported as mean titers with standard deviations for three independent experiments.

Vero virus. These data demonstrate that the N117D HA2 mutation is primarily responsible for Vero cell adaptation.

Generation of a high-growth vaccine seed virus in Vero cells. Based on a National Center for Biotechnology Information (NCBI) database search, more than 99% of viruses possess asparagine at position 117 (H1 subtype) or 116 (H3 subtype) of HA2. Asparagine at this position is located in the α-helix of the stalk region of the HA molecule, which is close to the viral membrane surface (Fig. 2A). We therefore sought to determine whether the HA2 N117D (or N116D) amino acid substitution could enhance the growth of other viruses in Vero cells. To this end, we introduced the HA2 N117D or N116D mutation into the HAs of the H1 seasonal strains A/Kawasaki/173/01 (H1N1) and A/Kawasaki/UTK-4/09 (H1N1), the pandemic strain A/California/4/2009 (H1N1), and the H3 seasonal strain A/Yokohama/2013/2003 (H3N2). We then generated PR8/H1N1 or PR8/H3N2 6:2 reassortants with these mutated HAs by using reverse genetics. We also produced 6:2 reassortants with wild-type HA from each virus for comparison. Each virus possessing mutated HA grew to a 100 to 1,000 times higher titer than its wild-type HA-bearing counterpart in Vero cells (Fig. 2C). In contrast, we did not observe any marked differences in virus titers between wild-type and mutant reassortants in MDCK cells (data not shown). These data suggest that the HA2 N117(116)D mutation would universally enhance the growth of a vaccine seed virus in Vero cells.

The HA2 N117D mutation alters the pH range for virus membrane fusion. Since the HA2 region mediates virus membrane fusion and the HA2 N117 residue is located close to the fusion peptide (Fig. 2B), we examined whether the mutation affects the optimal pH for viral membrane fusion. We constructed plasmids expressing PR8 wild-type HA or HA2 N117D mutant HA and transfected them into Vero cells. A GFP expression plasmid was cotransfected into the cells for a fusion assay. At 24 h posttransfection, we treated the cells with several low-pH buffers and observed fused cells (Fig. 3). At neutral pH (pH 7.4), we did not observe any fused cells with either wild-type HA or N117D mutant HA-transfected Vero cells. At pH 5.0 and 5.2, numerous fused cells were observed in both wild-type HA and mutant HA-transfected cells. Interestingly, at pH 5.4, few fused cells were observed in wild-type HA-transfected cells, whereas many fused cells were observed in mutant N117D HA-transfected cells. At pH 5.6, both wild-type HA and mutant HA-transfected cells produced limited cell-cell fusion. In addition to the change in optimal pH for membrane fusion in mutant HA-expressed fused cells, the

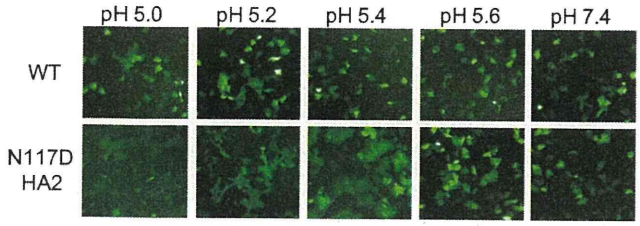

FIG 3 Syncytium formation of Vero cells expressing WT PR8 and HA2 N117D mutant HAs. Vero cells were cotransfected with WT HA or a mutant HA expression plasmid and with a GFP expression plasmid. After treatment with the indicated pH buffers, the cells were observed under a fluorescence microscope.

number of cells involved in cell-cell fusion was greater in these cells than in wild-type HA-transfected cells, even at pH 5.0 and 5.2. We also performed cell fusion assays in MDCK cells with wild-type and mutant HAs, and the results were very similar to those obtained in Vero cells (data not shown). These data indicate that the HA2 N117D mutation both augments membrane fusion and widens the optimal pH range for virus membrane fusion in Vero cells.

Comparison of endosomal pH between Vero and MDCK cells. Although wild-type PR8 virus growth is suboptimal in Vero cells, wild-type PR8 grew to a level comparable to that of HA2 N117D mutants in MDCK cells (Fig. 4A). The optimal pH for viral membrane fusion was higher for the HA2 N117D mutant than for the wild type (Fig. 3), allowing us to hypothesize that the endosomal pH of Vero cells is higher than that of MDCK cells. To test this hypothesis, we compared the endosomal pH between Vero and MDCK cells by introducing dextran-conjugated fluorescent dye as a marker and measuring the intracellular intensity (Fig. 4A). This assay is based on the principle that the fluorescence intensity of Oregon green 488 is sensitive to low pH whereas the intensity of Alexa Fluor 647 is not pH sensitive (25). Thus, pHs can be compared by measuring the intensity of each fluorescent dye and calculating the intensity ratio between Alexa Fluor 647 and Oregon green 488. Vero and MDCK cells were incubated with Alexa Fluor 647- and Oregon green 488-conjugated dextran for 15 min at 37°C. After incubation, the cells were washed and the intensities of Alexa Fluor 647 and Oregon green 488 were measured by using confocal microscopy. The Oregon green 488/Alexa Fluor 647 intensity ratio was appreciably higher in Vero cells than in MDCK cells (Fig. 4B), suggesting that the early endosomal pH value is higher in Vero cells than in MDCK cells.

DISCUSSION

Here, we described an approach to enhance the growth of influenza vaccine seed viruses in Vero cells, which are approved for use in human vaccine production. Influenza vaccine seed viruses that provide robust growth in cell culture are needed to ensure an adequate supply of influenza vaccines as either a supplement to or an alternative method for egg-based vaccine production. Our approach involved introducing a single amino acid mutation (N117D) into the HA2 subunit of HA, which was found in a Vero cell-adapted PR8 virus. The seasonal influenza vaccine seed-like viruses (6:2 reassortants with a PR8 backbone) tested in this study grew poorly in Vero cells. However, the introduction of this HA2 single mutation into these viruses produced mutants that grew to 100 to 1,000 times higher titers in Vero cells than wild-type viruses. This strategy for virus growth enhancement based on the HA2 mutation could thus be feasible for the production of growth-enhanced seasonal or pandemic vaccine seed viruses.

The amino acid at position 117 of HA2 is located on the stem region of HA. One concern is the possibility that changing the amino acid residue at this position may affect the antigenicity of inactivated vaccines, although the major antigenic sites of H1 HA (Ca, Cb, Sa, and Sb), against which most neutralization antibodies elicited by inactivated vaccines are raised, are located on the globular head region that surrounds the receptor binding site (3). Recent studies revealed that antibodies against the HA stem region confer universal protection from influenza virus infection (5, 9, 17, 39, 40). However, such neutralizing antibodies are rarely induced by conventional vaccinations (28). These findings suggest that the HA2 N117D mutation would not affect the antigenicity or efficacy of the vaccines.

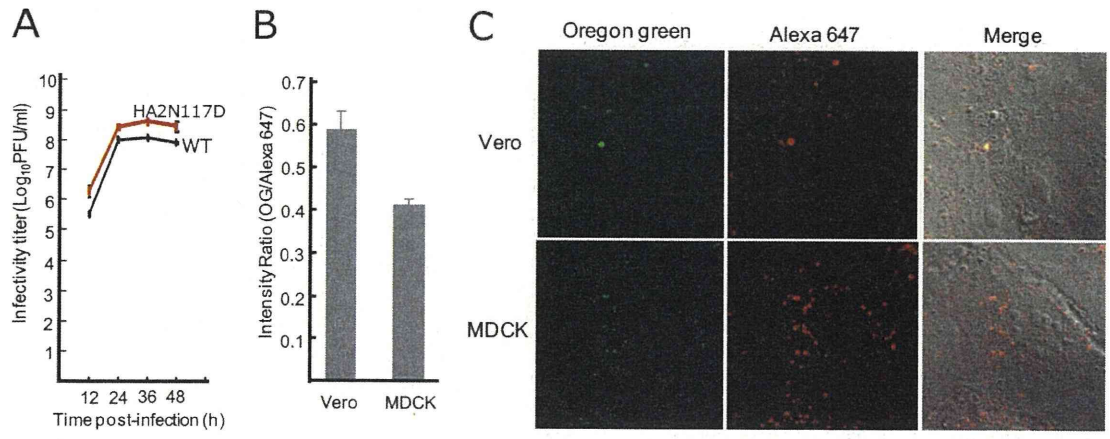

FIG 4 Comparison of endosomal pHs between Vero and MDCK cells. (A) Growth kinetics of WT PR8 and HA2 N117D mutant viruses in MDCK cells. The infectivity titers of WT and mutant viruses were determined following inoculation at an MOI of 0.01. The data are reported as mean titers with standard deviations for three independent experiments. (B) Oregon green (OG)-conjugated dextran (250 μg/ml) and Alexa 647-conjugated dextran (30 μg/ml) were internalized. After 15 min, fluorescence intensities were measured by using confocal microscopy and calculated as OG/Alexa 647 ratios. The data are reported as mean values with standard deviations obtained for five microscopic fields for each cell culture. (C) Representative microscopic images corresponding to panel B.

Here, we suggest that the growth enhancement was most likely due to broadening of the optimal pH range for virus membrane fusion mediated by HA2. The mutation site is located in the HA stalk region, close to the fusion peptide in the HA trimer (Fig. 2B). To accomplish virus membrane fusion, cleaved HA needs to be exposed to low pH (14). Previous reports demonstrate that the substitution of the neutral amino acid residue(s) in the HA stalk region for charged amino acids affects the optimal pH for virus membrane fusion (24, 32, 33, 43). Since the N117D substitution introduces a negative charge, it may change the electrostatic balance between the residue at position 117 and the fusion peptide, possibly resulting in fewer proton-dependent conformational changes in the HA molecule.

We revealed that the endosomal pH was higher in Vero cells than in MDCK cells 15 min after dextran intake. Based on this observation, we assume that this difference in endosomal pH affects virus growth in these cell lines. Indeed, cell-type-dependent endosomal pH kinetics are important for influenza virus infection (21, 22). In MDCK cells, influenza virus reaches the late endosome (pH 5.0) 10 min after endocytosis (21). On the other hand, in HeLa cells, which is a nonpermissive cell line for influenza virus infection (6), it takes 40 min for influenza virus to colocalize with a late endosome marker following endocytosis (36). However, highly pathogenic H5N1 virus, which requires a higher pH for optimal membrane fusion (pH 5.9) (32), grows in MDCK, Vero, and HeLa cells with comparable titers (44). Moreover, vesicular stomatitis virus (VSV) infectivity is much lower in MDCK cells than in Vero cells (11), possibly due to the higher optimal pH (pH 6.0) for membrane fusion of the VSV G protein (34). These facts imply that Vero cells may have a higher pH in the early endosome than MDCK cells. A precise assessment of endosomal pH changes is needed to better understand the mechanism of enhanced virus growth in Vero cells.

We used PR8 virus as a reassortant backbone virus in this study because it is attenuated in humans and is approved by the WHO for use as a genetic backbone for vaccine seed viruses (42). However, introducing the HA2 mutation identified here into any wild-type virus, including seasonal influenza viruses, could also enhance virus replication in Vero cells, providing alternative vaccine seed viruses for the production of inactivated influenza vaccines.

In conclusion, we propose a mutant virus possessing aspartic acid at HA2 position 117 as a seed virus for Vero cell-based influenza vaccine production. A virus with this single amino acid mutation can be produced easily by using reverse genetics. A cell culture-based vaccine strategy with this seed virus would allow the production of more doses of inactivated influenza vaccines in a timely, cost-effective manner, not only for seasonal, but also for pandemic vaccines.

ACKNOWLEDGMENTS

We thank Y. Kino (Chemo-Sero-Therapeutic Research Institute, Japan) for Vero WCB cells and S. Watson for scientific editing.

This work was supported in part by Grants-in-Aid for Specially Promoted Research and for Scientific Research (B); by a contract research fund from the Ministry of Education, Culture, Sports, Science and Technology of Japan; by the Program of Founding Research Centers for Emerging and Reemerging Infectious Diseases; by Grants-in-Aid for Specially Promoted Research and for Scientific Research; by ERATO (Japan Science and Technology Agency); and by National Institute of Allergy and Infectious Diseases Public Health Service research grants.

REFERENCES

1. Barrett PN, et al. 2011. Efficacy, safety, and immunogenicity of a Vero-cell-culture-derived trivalent influenza vaccine: a multicentre, double-blind, randomised, placebo-controlled trial. Lancet 377:751–759.
2. Barrett PN, Mundt W, Kistner O, Howard MK. 2009. Vero cell platform in vaccine production: moving towards cell culture-based viral vaccines. Expert Rev. Vaccines 8:607–618.
3. Brownlee GG, Fodor E. 2001. The predicted antigenicity of the haemagglutinin of the 1918 Spanish influenza pandemic suggests an avian origin. Philos. Trans. R. Soc. Lond. B Biol. Sci. 356:1871–1876.
4. Clark TW, et al. 2009. Trial of 2009 influenza A (H1N1) monovalent MF59-adjuvanted vaccine. N. Engl. J. Med. 361:2424–2435.
5. Corti D, et al. 2010. Heterosubtypic neutralizing antibodies are produced by individuals immunized with a seasonal influenza vaccine. J. Clin. Invest. 120:1663–1673.
6. De BK, Nayak DP. 1980. Defective interfering influenza viruses and host cells: establishment and maintenance of persistent influenza virus infection in MDBK and HeLa cells. J. Virol. 36:847–859.
7. Ehrlich HJ, et al. 2009. A cell culture (Vero)-derived H5N1 whole-virus vaccine induces cross-reactive memory responses. J. Infect. Dis. 200: 1113–1118.
8. Ehrlich HJ, et al. 2008. A clinical trial of a whole-virus H5N1 vaccine derived from cell culture. N. Engl. J. Med. 358:2573–2584.
9. Ekiert DC, et al. 2009. Antibody recognition of a highly conserved influenza virus epitope. Science 324:246–251.
10. Genzel Y, Fischer M, Reichl U. 2006. Serum-free influenza virus production avoiding washing steps and medium exchange in large-scale microcarrier culture. Vaccine 24:3261–3272.
11. Green RF, Meiss HK, Rodriguez-Boulan E. 1981. Glycosylation does not determine segregation of viral envelope proteins in the plasma membrane of epithelial cells. J. Cell Biol. 89:230–239.
12. Gupta RK, and Nguyen-Van-Tam JS. 2006. Oseltamivir resistance in influenza A (H5N1) infection. N. Engl. J. Med. 354:1423–1424.
13. Halperin SA, et al. 2002. Safety and immunogenicity of a trivalent, inactivated, mammalian cell culture-derived influenza vaccine in healthy adults, seniors, and children. Vaccine 20:1240–1247.
14. Harrison SC. 2008. Viral membrane fusion. Nat. Struct. Mol. Biol. 15: 690–698.
15. Horimoto T, et al. 2007. Enhanced growth of seed viruses for H5N1 influenza vaccines. Virology 366:23–27.
16. James JM, et al. 1998. Safe administration of influenza vaccine to patients with egg allergy. J. Pediatr. 133:624–628.
17. Kashyap AK, et al. 2008. Combinatorial antibody libraries from survivors of the Turkish H5N1 avian influenza outbreak reveal virus neutralization strategies. Proc. Natl. Acad. Sci. U. S. A. 105:5986–5991.
18. Katz JM, Webster RG. 1992. Amino acid sequence identity between the HA1 of influenza A (H3N2) viruses grown in mammalian and primary chick kidney cells. J. Gen. Virol. 73:1159–1165.
19. Keitel WA, et al. 2009. Safety and immunogenicity of inactivated, Vero cell culture-derived whole virus influenza A/H5N1 vaccine given alone or with aluminum hydroxide adjuvant in healthy adults. Vaccine 27: 6642–6648.
20. Kobasa D, et al. 2004. Enhanced virulence of influenza A viruses with the haemagglutinin of the 1918 pandemic virus. Nature 431:703–707.
21. Lakadamyali M, Rust MJ, Babcock HP, Zhuang X. 2003. Visualizing infection of individual influenza viruses. Proc. Natl. Acad. Sci. U. S. A. 100:9280–9285.
22. Lakadamyali M, Rust MJ, Zhuang X. 2004. Endocytosis of influenza viruses. Microbes Infect. 6:929–936.
23. Le QM, et al. 2005. Avian flu: isolation of drug-resistant H5N1 virus. Nature 437:1108.
24. Lin YP, et al. 1997. Adaptation of egg-grown and transfectant influenza viruses for growth in mammalian cells: selection of hemagglutinin mutants with elevated pH of membrane fusion. Virology 233:402–410.
25. Marchetti A, Lelong E, Cosson P. 2009. A measure of endosomal pH by flow cytometry in Dictyostelium. BMC Res. Notes 2:7.
26. Montagnon BJ. 1989. Polio and rabies vaccines produced in continuous cell lines: a reality for Vero cell line. Dev. Biol. Stand. 70:27–47.
27. Murakami S, et al. 2008. Establishment of canine RNA polymerase I-driven reverse genetics for influenza A virus: its application for H5N1 vaccine production. J. Virol. 82:1605–1609.
28. Nabel GJ, Fauci AS. 2010. Induction of unnatural immunity: prospects

for a broadly protective universal influenza vaccine. Nat. Med. 16: 1389–1391.
29. Neumann G, et al. 1999. Generation of influenza A viruses entirely from cloned cDNAs. Proc. Natl. Acad. Sci. U. S. A. 96:9345–9350.
30. Octaviani CP, Ozawa M, Yamada S, Goto H, Kawaoka Y. 2010. High level of genetic compatibility between swine-origin H1N1 and highly pathogenic avian H5N1 influenza viruses. J. Virol. 84:10918–10922.
31. Ozawa M, Goto H, Horimoto T, Kawaoka Y. 2007. An adenovirus vector-mediated reverse genetics system for influenza A virus generation. J. Virol. 81:9556–9559.
32. Reed ML, et al. 2010. The pH of activation of the hemagglutinin protein regulates H5N1 influenza virus pathogenicity and transmissibility in ducks. J. Virol. 84:1527–1535.
33. Reed ML, et al. 2009. Amino acid residues in the fusion peptide pocket regulate the pH of activation of the H5N1 influenza virus hemagglutinin protein. J. Virol. 83:3568–3580.
34. Roche S, Bressanelli S, Rey FA, Gaudin Y. 2006. Crystal structure of the low-pH form of the vesicular stomatitis virus glycoprotein G. Science 313:187–191.
35. Rybak SL, Murphy RF. 1998. Primary cell cultures from murine kidney and heart differ in endosomal pH. J. Cell Physiol. 176:216–222.
36. Sieczkarski SB, Whittaker GR. 2003. Differential requirements of Rab5 and Rab7 for endocytosis of influenza and other enveloped viruses. Traffic 4:333–343.
37. Smith KA, Colvin CJ, Weber PS, Spatz SJ, Coussens PM. 2008. High titer growth of human and avian influenza viruses in an immortalized chick embryo cell line without the need for exogenous proteases. Vaccine 26:3778–3782.
38. Sugawara K, et al. 2002. Development of Vero cell-derived inactivated Japanese encephalitis vaccine. Biologicals 30:303–314.
39. Sui J, et al. 2009. Structural and functional bases for broad-spectrum neutralization of avian and human influenza A viruses. Nat. Struct. Mol. Biol. 16:265–273.
40. Wang TT, et al. 2010. Vaccination with a synthetic peptide from the influenza virus hemagglutinin provides protection against distinct viral subtypes. Proc. Natl. Acad. Sci. U. S. A. 107:18979–18984.
41. WHO. 1995. Cell culture as a substrate for the production of influenza vaccines: memorandum from a WHO meeting. Bull. World Health Organ. 73:431–435.
42. Wood JM, Robertson JS. 2004. From lethal virus to life-saving vaccine: developing inactivated vaccines for pandemic influenza. Nat. Rev. Microbiol. 2:842–847.
43. Xu R, Wilson IA. 2011. Structural characterization of an early fusion intermediate of influenza virus hemagglutinin. J. Virol. 85:5172–5182.
44. Yang W, Qu S, Liu Q, Zheng C. 2009. Avian influenza virus A/chicken/Hubei/489/2004 (H5N1) induces caspase-dependent apoptosis in a cell-specific manner. Mol. Cell Biochem. 332:233–241.

Vaccine 28 (2010) 780–789

Contents lists available at ScienceDirect

Vaccine

journal homepage: www.elsevier.com/locate/vaccine

Subcutaneous inoculation of a whole virus particle vaccine prepared from a non-pathogenic virus library induces protective immunity against H7N7 highly pathogenic avian influenza virus in cynomolgus macaques

Yasushi Itoh[a], Hiroichi Ozaki[e], Hirohito Ishigaki[a], Yoshihiro Sakoda[f], Tomoya Nagata[a,b], Kosuke Soda[f], Norikazu Isoda[f], Taichiro Miyake[a,c], Hideaki Ishida[a], Kiyoko Okamoto[a], Misako Nakayama[a], Hideaki Tsuchiya[d], Ryuzo Torii[d], Hiroshi Kida[f,g], Kazumasa Ogasawara[a,d,*]

[a] Department of Pathology, Shiga University of Medical Science, Otsu, Shiga 520-2192, Japan
[b] Department of Otorhinolaryngology-Head and Neck Surgery, Shiga University of Medical Science, Otsu, Shiga 520-2192, Japan
[c] Department of Ophthalmology, Shiga University of Medical Science, Otsu, Shiga 520-2192, Japan
[d] Research Center for Animal Life Science, Shiga University of Medical Science, Otsu, Shiga 520-2192, Japan
[e] Faculty of Agriculture, Tottori University, Tottori 680-8553, Japan
[f] Laboratory of Microbiology, Department of Disease Control, Graduate School of Veterinary Medicine, Hokkaido University, Sapporo 060-0818, Japan
[g] Research Center for Zoonosis Control, Hokkaido University, Sapporo 001-0020, Japan

ARTICLE INFO

Article history:
Received 1 June 2009
Received in revised form 9 September 2009
Accepted 13 October 2009
Available online 24 October 2009

Keywords:
H7N7
Highly pathogenic avian influenza virus
Non-human primate

ABSTRACT

Development of H7N7 highly pathogenic avian influenza virus (HPAIV) vaccines is an urgent issue since human cases of infection with this subtype virus have been reported and most humans have no immunity against H7N7 viruses. We made an H7N7 vaccine combining components from an influenza virus library of non-pathogenic type A influenza viruses. Antibody and T cell recall responses specific against the vaccine strain were elicited by subcutaneous inoculation with the whole virus particle vaccine with or without alum as an adjuvant in cynomolgus macaques. No significant difference was observed in magnitude of antibody responses between vaccination with alum and vaccination without alum, though vaccination with alum induced longer recall responses of $CD8^+$ T cells than did vaccination without alum. After challenge with a subtype of H7N7 HPAIV, the virus was detected in nasal swabs of unvaccinated macaques for 8 days but only for 1 day in the animals vaccinated either with or without alum, although the macaques vaccinated with alum showed elevated body temperature more briefly after infection. These findings demonstrated that this H7N7 HPAIV strain is pathogenic to macaques and that the vaccine conferred protective immunity to macaques against H7N7 HPAIV infection.

1. Introduction

H7 subtype influenza viruses fall into two geographically distinct lineages, Eurasian and North American [1]. The Eurasian lineage contains highly pathogenic avian influenza viruses (HPAIVs) that possess multibasic amino acids in hemagglutinin (HA) cleaved by not only trypsin-like enzymes but also other ubiquitous proteases, resulting in high mortality in poultry [2]. Of these, outbreaks of H7N7 HPAIV infection caused 89 human cases with conjunctivitis in the Netherlands in 2003, including one fatal case. More than 50% of the infected people had serum antibodies after recovery that reacted with H7N7 virus [3,4]. The recent increase in findings of H7 avian influenza viruses from outbreaks in poultry and humans has raised concerns about the possibility of additional zoonotic transmissions of influenza viruses from poultry to humans, which would pose a public health threat [5,6]. In addition, H7 influenza viruses from the North American lineage have acquired sialic acid-binding properties that closely resemble those in human influenza viruses, and are transmissible in the ferret model [7]. These findings suggest that H7 HPAIVs may become transmissible in humans. Since most people have no immunity against H7 influenza viruses, development of vaccines against H7 subtype viruses is an urgent issue [8–10].

In a similar study on H5 vaccination, we previously demonstrated that formalin-inactivated whole virus particle vaccines induced protective immune responses including antibody and cytotoxic T lymphocyte (CTL) responses in mice and that the whole virus particle vaccines conferred protective immunity against H5N1 HPAIV challenge in cynomolgus macaques [11,12]. Although the unvaccinated cynomolgus macaques infected with H5N1 HPAIV

* Corresponding author at: Department of Pathology, Shiga University of Medical Science, Setatsukinowa, Otsu, Shiga 520-2192, Japan. Tel.: +81 77 548 2171; fax: +81 77 548 2423.
E-mail address: maruichi@belle.shiga-med.ac.jp (K. Ogasawara).

0264-410X/$ – see front matter © 2009 Elsevier Ltd. All rights reserved.
doi:10.1016/j.vaccine.2009.10.067

did not die as did ferrets and mice [13–16], H5N1 HPAIV was detected for 5 days after challenge with H5N1 HPAIV, a duration sufficient to assess the effects of vaccines. Indeed, H5N1 HPAIV was recovered from the vaccinated macaques only for 1 day after challenge with the virus. Hence, we believe that prevention of virus replication in animals is a more reliable indicator of vaccine efficacy than is prevention of death. This is especially true when using mice, since most laboratory mice possess a defective version of the *Mx* gene related to prevention of virus replication in humans and it may be difficult to determine the degree of vaccination effect when using survival rates alone [17]. The macaque model allowed us better to analyze pathogenicity of HPAIV and the effects of vaccines for preclinical studies.

In this H7N7 study, we made a non-pathogenic H7N7 virus vaccine using two strains from a virus library of 144 different combinations of 16 HA and 9 neuraminidase (NA) subtypes of non-pathogenic viruses [18]. One parental strain, A/duck/Mongolia/736/2002 (H7N7), is non-pathogenic in chickens, but its growth potential in embryonated eggs is insufficient for vaccine manufacture. Therefore, we selected A/duck/Hokkaido/49/1998 (H9N2), which has better growth potential in embryonated eggs and is likewise not pathogenic in chickens, as a partner for the genetic reassortment to obtain a vaccine strain [10,19]. The product was grown and inactivated to make a whole virus particle vaccine as described previously [10,19]. At first, we examined immune responses induced by subcutaneous inoculation with the inactivated whole virus particle vaccine. Next, we examined the pathogenicity of the H7N7 HPAIV in cynomolgus macaques to establish a non-human primate model for assessing vaccine efficacy and subsequent protection against an H7N7 HPAIV by vaccination.

We also examined the effects of an adjuvant, alum (aluminum hydroxide), in combination with the whole virus particle vaccine. Alum has been used in vaccines for humans [20–22] and is considered to enhance Th2 type responses [23]. Indeed, it was recently demonstrated that alum activated the Nalp3 inflammasome pathway, resulting in production of pro-inflammatory cytokines IL-1β and IL-18 and that Nalp3-deficient mice failed to mount a significant antibody response to an antigen administered with alum [24–26]. In contrast to the results of some studies, we found that alum with the H7N7 whole virus particle vaccine induced not only antigen-specific antibody responses but also $CD8^+$ T cell responses in cynomolgus macaques. Furthermore, the vaccine with alum conferred $CD8^+$ T cell recall responses for a longer period than without alum, although alum did not affect the period of virus replication in the nasal cavity, trachea, or bronchus.

2. Materials and methods

2.1. Viruses

For a vaccine, we used the influenza virus A/duck/Hokkaido/Vac-2/2004 (H7N7) (Vac-2, National Center for Biotechnology Information (NCBI) taxonomy database ID: 390987); this is a genetic reassortant generated by coinfection with A/duck/Mongolia/736/2002 (H7N7) and A/duck/Hokkaido/49/1998 (H9N2) in chicken embryos. The PB2, PB1, PA, HA, NA, and the NS genes of Vac-2 were derived from the H7N7 virus, and NP and M genes were derived from the H9N2 virus [10].

For our test (challenge) pathogen, an HPAIV, A/chicken/Netherlands/2586/2003 (H7N7) (NL2586, NCBI taxonomy database ID: 533037), was provided by Dr. I. Capua (L'Office International des Épizooties (OIE), Food and Agriculture Organization of the United Nations (FAO), and National Reference Laboratory for Newcastle Disease and Avian Influenza, Istituto Zooprofilattico Sperimentale delle Venezie, Italy) [10,27]. The amino acid sequence identities between Vac-2 and NL2586 were 97% in HA and 98% in NA.

Both the Vac-2 viruses for vaccine and the NL2586 for challenge to macaques were propagated in allantoic cavities of 10-day-old embryonated hen's eggs at 35 °C for 48 h. To prepare an inactivated vaccine, the Vac-2 infected allantoic fluids were concentrated and purified by high-speed centrifugation (112,500 × *g* for 90 min) through a 10–50% sucrose density gradient and then treated in 0.1% formalin at 4 °C for 1 week [10]. The amount of whole particle vaccines was indicated as that of entire protein including HA and the other viral proteins. The vaccine used in the present study contained 42,667 HA units in 1 mg vaccine.

In order to assess virus replication, serial dilutions of swabs and whole blood samples were inoculated onto confluent Madin–Darby canine kidney (MDCK) cells as described previously [11]. Cytopathic effects were then examined under a microscope 72 h later.

2.2. Animals

Five- to seven-year-old cynomolgus macaques (*Macaca fascicularis*) were used with permission of the Shiga University of Medical Science Animal Experiment Committee and Biosafety Committee. Cynomolgus macaques in the present study were healthy young adults old enough for pregnancy. In the text and figures, individual macaques are distinguished by identification numbers. The absence of H7N7-specific antibodies in their sera was confirmed before experiments using antigen-specific enzyme-linked immunosorbent assays (ELISA). Under anesthesia 2 weeks before virus inoculation, a telemetry probe (TA10CTA-D70, Data Sciences International, St. Paul, MN) was implanted in the peritoneal cavity of each macaque to monitor body temperature. The macaques used in this study were free from B virus, hepatitis E virus, *Mycobacterium tuberculosis*, *Shigella* spp., *Salmonella* spp., and *Entamoeba histolytica* [11].

The vaccine (1 mg/dose) was inoculated subcutaneously into macaques using syringes with and without alum (500 μl, Superfos Biosector, Vaerloese, Denmark) twice with a 2-week interval between injections. Saline instead of the vaccine was inoculated into macaques as unvaccinated controls. The macaques were challenged with NL2586 (2×10^7 $TCID_{50}$) on the conjunctiva (1×10^6 $TCID_{50}$/50 μl for each eye) and into nasal cavities (9×10^6 $TCID_{50}$/450 μl for each nasal cavity) with pipettes 10 weeks after the second vaccination. Experiments using NL2586 were performed in the biosafety level 3 facility of the Research Center for Animal Life Science, Shiga University of Medical Science.

Under anesthesia, two cotton sticks (TE8201, Eiken Chemical, Ltd., Tokyo, Japan) were used to collect fluid samples in nasal cavities and tracheas, and the sticks were subsequently immersed in 1 ml of PBS containing 0.1% BSA and antibiotics. A bronchoscope (MEV-2560, Machida Endoscope Co., Ltd., Tokyo, Japan) and brushes (BC-203D-2006, Olympus, Tokyo, Japan) were used to collect bronchial samples [28]. The brushes were quickly immersed in 1 ml of PBS containing BSA and antibiotics.

2.3. Antibody assays

The antibody titers of serum and swab samples against Vac-2 antigens were determined using ELISA [29]. For ELISA, 96-well plates were coated with 50 μl of purified Vac-2 (20 μg/ml) disrupted with 0.05 M Tris–HCl (pH 7.8) containing 0.5% Triton X-100 and 0.6 M KCl. Serially diluted samples were incubated overnight in the coated plates. After washing five times, horseradish peroxidase-conjugated anti-monkey IgG antibodies (MP Biomedicals, Inc./Cappel, Aurora, OH) (1:1000 × 50 μl) or anti-monkey IgA antibodies (Nordic Immunological Laboratories, Tilburg, The Netherlands) (1:4000 × 50 μl) were added and incubated for 1 h at room temperature. Horseradish peroxidase activity was assessed using 3,3′,5,5′-tetramethyl benzidine substrate (100 μl). The reac-

tion was stopped by the addition of 1 M hydrogen chloride (100 μl). Optical density was measured at 450 nm.

2.4. Virus neutralization assay

The serum samples were pretreated with receptor destroying enzyme (RDEII, Denka Seiken, Tokyo, Japan) at 37 °C overnight and then inactivated at 56 °C for 1 h. Diluted samples were mixed with 50 $TCID_{50}$ of viruses for 1 h. Then the mixture was added onto an MDCK monolayer. After 1-h incubation, the suspension was removed, and the cells were cultured in MEM containing 0.1% BSA and 5 μg/ml trypsin. After incubation at 35 °C for 3 days, the number of wells with cytopathic effects was counted in quadruplicate culture. Neutralization titers were expressed as the dilution in which cytopathic effects were observed in 50% of the wells.

2.5. Hemagglutination-inhibition (HI) test

Serum samples were pretreated as described in Section 2.4. Serially diluted sera were mixed with 8 HA units of Vac-2 or NL2586 virus antigen for 1 h at room temperature. The mixture was then incubated with chicken red blood cells. After 30-min incubation, the HI titers were determined.

2.6. Cell proliferation

Lymphocytes were purified from peripheral blood of the macaques using a density gradient (Wako Pure Chemical Industries Ltd., Osaka, Japan). After washing, $CD8^+$ cells were isolated using CD8 microbeads for non-human primates and magnetic cell sorting (MACS, Miltenyi Biotec GmbH, Bergisch Gladbach, Germany), followed by separation of $CD4^+$ cells using CD4 microbeads. The purity of the isolated $CD4^+$ and $CD8^+$ population was confirmed after flow cytometry to be more than 90%. The cells remaining after removal of $CD4^+$ and $CD8^+$ cells were used as antigen-presenting cells (APC) after irradiation at 30 Gy. $CD4^+$ or $CD8^+$ T cells (1×10^5/well) and APC (0.5×10^5/well) were cultured with inactivated whole particle Vac-2 antigens in 96-well U-bottom plates for 72 h. [^{3}H]-Thymidine (0.5 μCi/well) was added for the last 16 h of culture. Incorporation of [^{3}H]-Thymidine was measured.

3. Results

3.1. Antibody responses after inoculation of the inactivated whole virus particle vaccine prepared from a non-highly pathogenic H7N7 strain in the virus library

The vaccine was given twice to each macaque, and during a 10-week period between the second vaccination and challenge with H7N7 HPAIV we examined antibody and T lymphocyte responses in the vaccinated and non-vaccinated macaques on schedule as described in Fig. 1. The macaques showed no systemic symptoms after vaccination. No skin reaction at the site of injection was observed after inoculation with whole particle vaccines alone, though subcutaneous nodules without skin erosion or ulceration were observed at the site of injection in macaques vaccinated with alum.

Two weeks after the first vaccination and immediately before the second vaccination, serum IgG specific against Vac-2 antigen was detected in all vaccinated macaques (data not shown), and serum levels of IgG antibodies specific against the H7N7 vaccine antigens reached a maximum in all of the macaques inoculated with inactivated Vac-2 with or without alum by 4 weeks after the second vaccination (Fig. 2a). Antigen-specific IgG antibodies were detected in nasal and tracheal swabs from all the vaccinated macaques except in the nasal swabs of #466 and in the tracheal swabs of #459 (Fig. 2c and e). Antigen-specific IgA was detected in sera from two macaques vaccinated without alum (#459 and #579) and in the nasal and tracheal swabs from one macaque vaccinated with inactivated Vac-2 with alum (#545) (Fig. 2b, d, and f).

Table 1
Hemagglutination-inhibition activities of serum samples after vaccination.

Vaccination	Animal	Antigen							
		Vac-2				NL2586			
		Week							
		4	6	8	10	4	6	8	10
Vac-2	409	256	128	64	64	<4	<4	<4	<4
	459	64	32	16	16	<4	<4	<4	<4
	579	256	128	64	32	<4	<4	<4	<4
Vac-2 + alum	414	256	128	32	16	<4	<4	<4	<4
	466	256	128	64	32	<4	<4	<4	<4
	545	128	64	32	32	<4	<4	<4	<4

Week: weeks after the first vaccination ('week 4' means 2 weeks after the second vaccination). Detection limit is 1:4. The difference between Vac-2 alone and Vac-2 with alum is not significant ($P > 0.05$).

In order to compare the duration of antibody responses between macaques vaccinated with alum and without alum, the serum HI activities were examined periodically (Table 1). HI activity against Vac-2 was observed in sera from macaques vaccinated with Vac-2 alone and Vac-2 with alum 2 weeks after the second vaccination, whereas no HI activity against the highly pathogenic strain NL2586 was ever detected. HI activity against Vac-2 in sera gradually declined after 4 weeks. However, the sera from vaccinated macaques 8 weeks after the second vaccination showed activity in neutralizing infectivity of Vac-2 virus and less potent but significant neutralization activity against the highly pathogenic strain NL2586, compared with those from unvaccinated macaques (Table 2). It is known that HI tests do not accurately detect neutralizing antibodies, especially when avian influenza viruses are used as HA antigens [29–31]. Therefore, the results of neutralization activity suggest induction of antibodies against NL2586 by vaccination with the whole particles of inactivated Vac-2. Furthermore, addition of alum did not show significant enhancement of the HI activity and neutralization activities.

IgG antibody responses specific for Vac-2 antigens in the nasal swabs were examined 10 weeks after the second vaccination (Fig. 3). Both the macaques vaccinated with alum and those vac-

Table 2
Neutralization of Vac-2 and NL2586 with sera obtained after the second vaccination.

Vaccination	Animal	50% neutralization titer (log 2)	
		Virus	
		Vac-2	NL2586
Saline	416	<2	<2
	421	<2	<2
	450	<2	<2
Vac-2	409	8.00	4.50
	459	7.23	2.33
	579	7.67	3.50
Vac-2 + alum	414	8.23	2.50
	466	9.18	3.00
	545	7.83	4.50

Cynomolgus macaques were immunized with Vac-2 as described in Fig. 2. Sera were collected 8 weeks after the second vaccination (10 weeks after the first vaccination). The averages of 50% neutralization titers against Vac-2 were 7.67 and 8.53 in sera from macaques vaccinated with Vac-2 alone and macaques vaccinated with Vac-2 with alum, respectively. P values with Student's t-test are 0.003 (saline vs. Vac-2 alone) and 0.03 (saline vs. Vac-2 with alum) when 50% neutralization titers below 2 are calculated as 2.

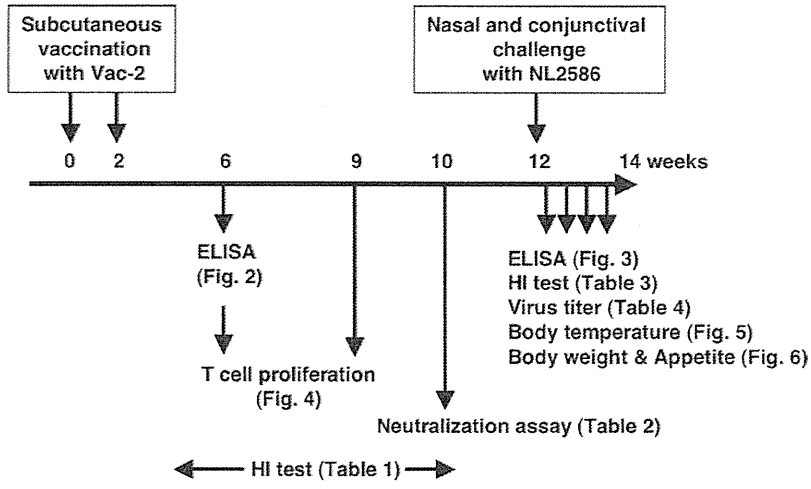

Fig. 1. Experimental schedule of the H7N7 vaccination and challenge in cynomolgus macaques. Cynomolgus macaques were subcutaneously immunized with whole virus particle vaccines of Vac-2 (1 mg/dose) without alum or with alum twice with a 2-week interval between injections. Blood and swab samples were collected after vaccination to examine antibody responses. Peripheral blood cells were used for proliferation assay in the 6th and 9th weeks. Neutralization assay was performed using sera collected in the 10th week. Ten weeks after the second vaccination, macaques were inoculated with HPAIV NL2586 onto conjunctivas and into nasal cavities. Swab samples were collected after inoculation with virus for virus titration. Body temperature, weight, and food consumption were recorded.

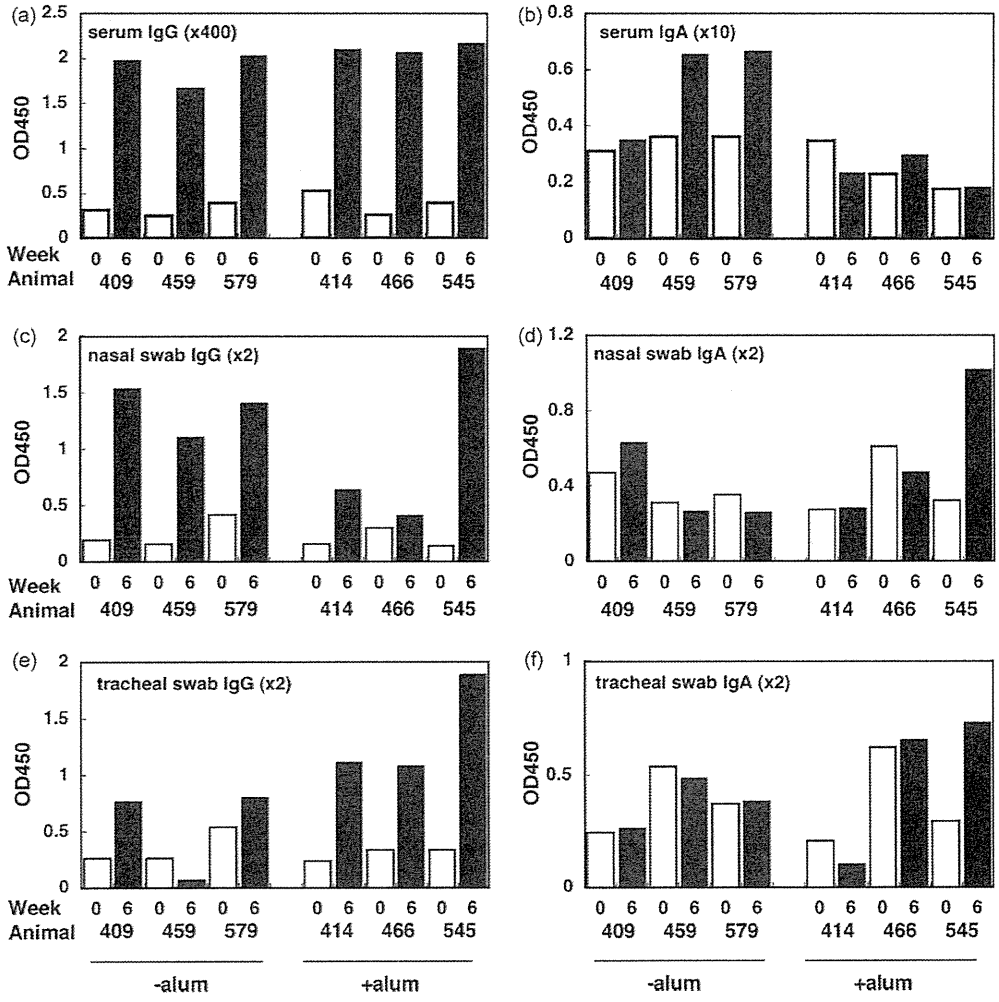

Fig. 2. Antibody responses specific against H7N7 vaccine antigens in cynomolgus macaques immunized with whole virus particle vaccines. Cynomolgus macaques were subcutaneously immunized with whole virus particle vaccines of Vac-2 without alum (#409, #459, and #579) or with alum (#414, #466, and #545). Four weeks after the second vaccination, sera and swabs were collected. IgG (a, c, and e) and IgA (b, d, and f) antibodies specific for Vac-2 antigens in sera (a and b), nasal swabs (c and d), and tracheal swabs (e and f) were analyzed at indicated dilutions using ELISA. Optical densities at 450 nm are shown. Open and filled bars indicate antibodies against Vac-2 antigens in pre-vaccinated samples and in samples 6 weeks after the first vaccination, respectively.

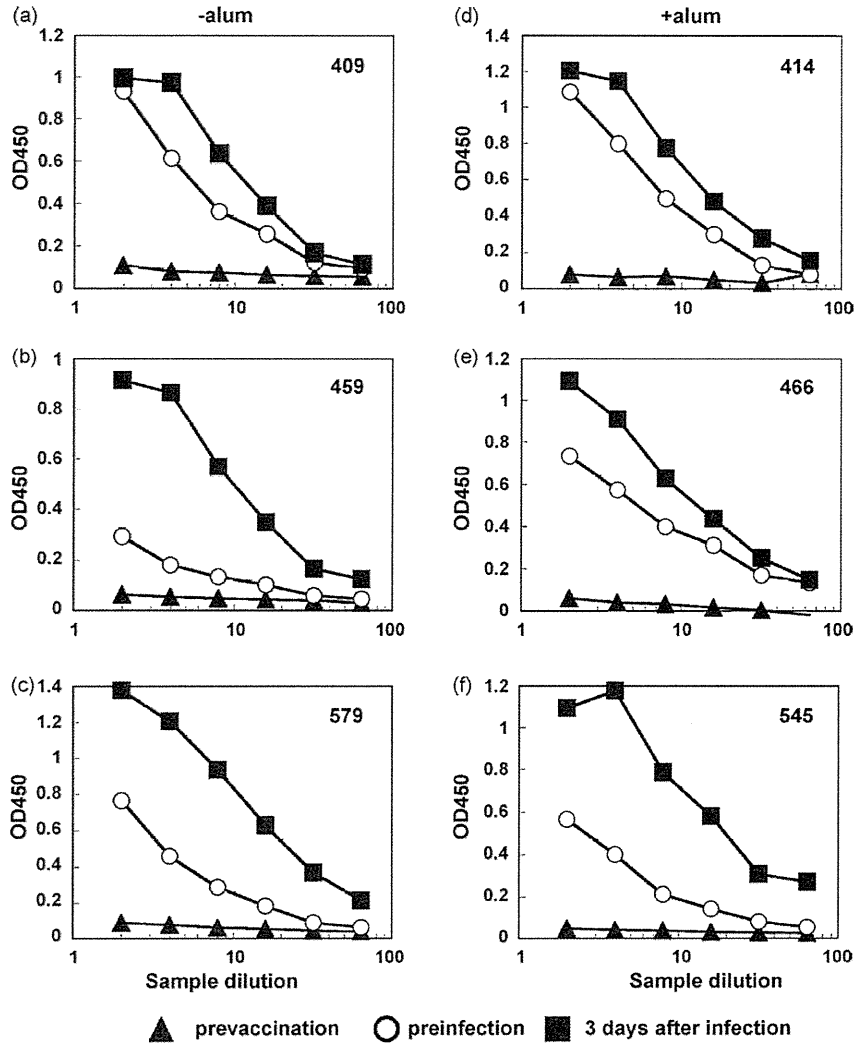

Fig. 3. Antibody responses specific against H7N7 vaccine antigens in cynomolgus macaques 10 weeks after vaccination and 3 days after the HPAIV challenge. Cynomolgus macaques were subcutaneously immunized with Vac-2 without alum (a–c) or with alum (d–f) as described in the legend of Fig. 2. Ten weeks after the second vaccination (open circle) and 3 days after the virus challenge (closed square), nasal swabs were collected. IgG antibodies specific against Vac-2 antigens were examined as described in Fig. 2. Closed triangles indicate antibodies against Vac-2 antigens in pre-vaccinated samples.

cinated without alum maintained high levels of IgG in nasal swabs, although one of the three macaques vaccinated without alum (#459) showed only a slight increase in IgG (Fig. 3b). In addition, recall responses of the antibodies detected 3 days after the virus challenge in the macaques vaccinated with alum were the same as those in the macaques vaccinated without alum (Fig. 3). Similarly, the levels of serum IgG antibodies specific for the Vac-2 antigens in all of the vaccinated macaques without alum at 10 weeks after the second vaccination were almost the same as the levels in the macaques vaccinated with alum (data not shown). Thus, alum did not affect the duration or intensity of antibody responses elicited by the vaccination.

3.2. T lymphocyte responses induced by whole virus particle vaccines prepared from a non-pathogenic H7N7 strain, Vac-2

T lymphocyte responses to Vac-2 antigens were assessed in peripheral blood of the macaques. $CD4^+$ and $CD8^+$ T lymphocytes in peripheral blood of the vaccinated animals were purified and cultured with the Vac-2 antigens (Fig. 4). Both $CD4^+$ and $CD8^+$ T lymphocytes obtained from three macaques inoculated with inactivated Vac-2 with alum 4 weeks after the second vaccination showed antigen-specific proliferation (Fig. 4a and b). $CD4^+$ and $CD8^+$ T lymphocytes obtained from two of the three macaques vaccinated without alum also showed antigen-specific proliferation. Proliferative responses of $CD4^+$ T lymphocytes obtained from the vaccinated macaques were seen 7 weeks after the second vaccination (Fig. 4c), whereas proliferative responses of $CD8^+$ T lymphocytes were elicited in cultures from the macaques vaccinated with alum but not from the macaques vaccinated without alum. Therefore, vaccination with alum evoked $CD8^+$ T lymphocyte recall responses for a longer period after vaccination than did vaccination without alum.

3.3. Pathogenicity of H7N7 HPAIV in cynomolgus macaques and protective effects of the inactivated whole virus particle vaccine

HPAIV NL2586 was inoculated on conjunctivas and in nasal cavities of macaques. Body temperature was expressed by calculating the average of the highest and lowest temperatures on 1 day, and the body temperature after the virus challenge was compared with that before the virus challenge. Higher body temperature than that before the challenge was observed for 11–13 days after inocula-

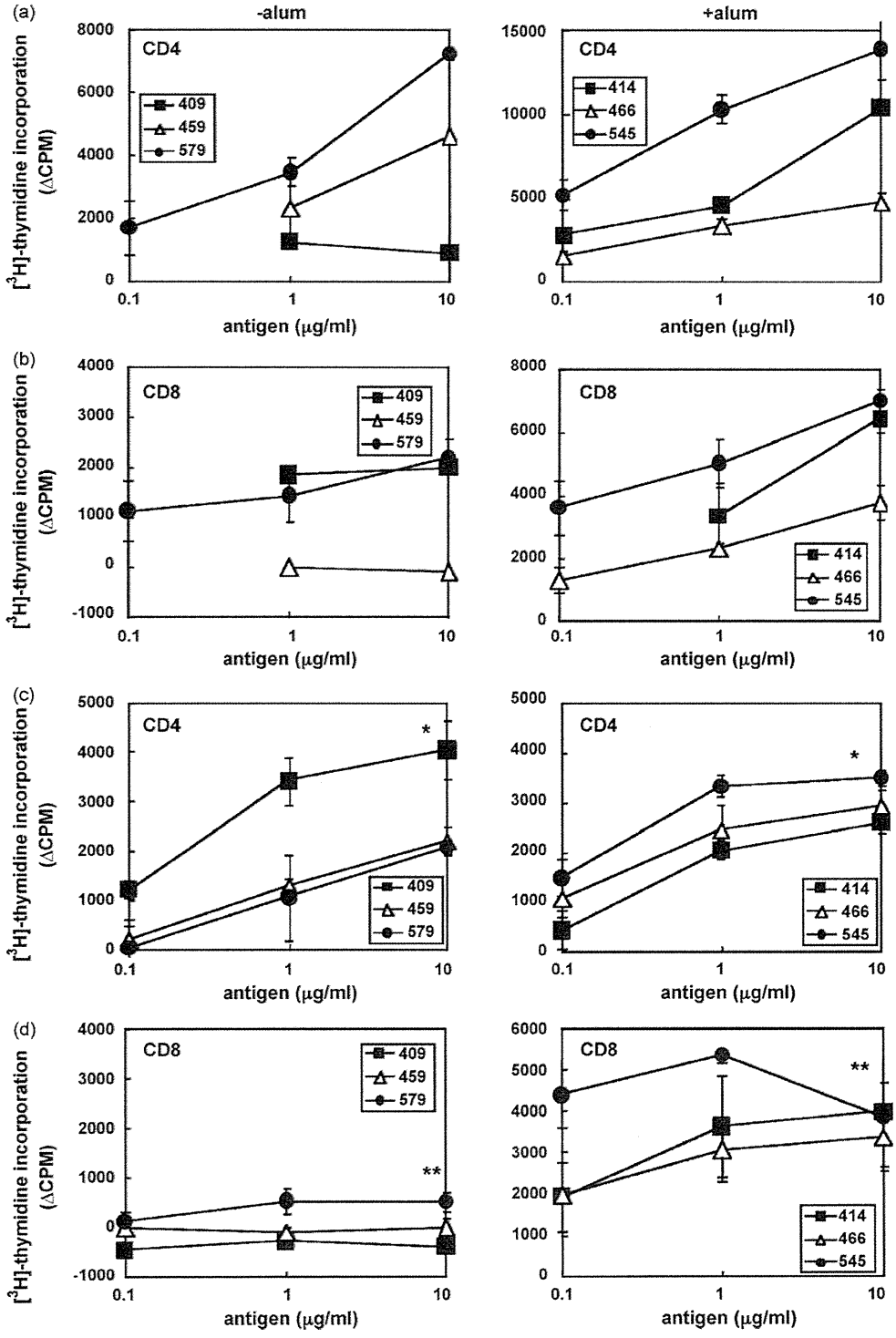

Fig. 4. $CD4^+$ and $CD8^+$ T lymphocyte proliferative responses specific for Vac-2 antigens. Cynomolgus macaques were subcutaneously immunized with Vac-2 without alum (left column) or with alum (right column) as described in the legend to Fig. 2. $CD4^+$ (a and c) and $CD8^+$ (b and d) lymphocytes were isolated from peripheral blood of the vaccinated macaques 4 weeks (a and b) and 7 weeks after the second vaccination (c and d). The differences of average proliferative responses of $CD4^+$ T cells are not significant between Vac-2 alone and Vac-2 with alum in (c) ($^*P > 0.05$). The differences of average proliferative responses of $CD8^+$ T cells are significant between Vac-2 alone and Vac-2 with alum in (d) ($^{**}P < 0.05$). T lymphocytes from macaques inoculated with saline did not show any proliferative responses against Vac-2 antigens (data not shown).

tion in the unvaccinated macaques (#416, #421, #450) (Fig. 5, left panels), while raised body temperature in the macaques vaccinated with inactivated Vac-2 alone was observed until day 7 (#579), day 9 (#459) and day 13 (#409) (Fig. 5, middle panels). Although the inactivated Vac-2 alone slightly decreased the duration of raised body temperature, inoculation of Vac-2 with alum considerably reduced the duration of raised body temperature to 4 days (Fig. 5, right panels). Therefore, these results indicate that vaccination with inactivated Vac-2, especially with alum, accelerated the recovery of body temperature.